METRICA
METRology Institutional CAtalog

ISTITUTO NAZIONALE DI RICERCA METROLOGICA
Repository Istituzionale

Barium gallo-germanate glasses co-activated with Cr3+/Er3+ and Cr3+/Er3+/Ln3+ (Ln = Yb, Ho) for near-infrared luminescence applications

Original
Barium gallo-germanate glasses co-activated with Cr3+/Er3+ and Cr3+/Er3+/Ln3+ (Ln = Yb, Ho) for near-infrared luminescence applications / Pisarski, W.A., Pisarska, J., Kuwik, M., Kochanowicz, M., Żmojda, J., Miluski, P., Dorosz, J., Pugliese, D., Wełna, M., Dorosz, D.. - In: SCIENTIFIC REPORTS. - ISSN 2045-2322. - 16:1(2026). [10.1038/s41598-026-65899-2]

Availability:
This version is available at: 11696/90499 since: 2026-10-26T06:45:25Z

Publisher:
Springer Nature

Published
DOI:10.1038/s41598-026-65899-2

Terms of use:

This article is made available under terms and conditions as specified in the corresponding bibliographic description in the repository

Publisher copyright

(Article begins on next page)

17 November 2026

scientific reports

Check for updates

OPEN

Barium gallo-germanate glasses co-activated with Cr^{3+}/Er^{3+} and $Cr^{3+}/Er^{3+}/Ln^{3+}$ (Ln = Yb, Ho) for near-infrared luminescence applications

Wojciech A. Pisarski[1]✉, Joanna Pisarska[1], Marta Kuwik[1], Marcin Kochanowicz[2], Jacek Żmojda[2], Piotr Miluski[2], Jan Dorosz[2], Diego Pugliese[3], Michał Wełna[4] & Dominik Dorosz[4]

Near-infrared luminescence properties of barium gallo-germanate glasses co-activated with Cr^{3+}/Er^{3+} and $Cr^{3+}/Er^{3+}/Ln^{3+}$ (Ln = Yb, Ho) have been studied for the first time. Compared to Cr^{3+}/Er^{3+} co-doped sample, near-infrared emission of Er^{3+} at 1534 nm in $Cr^{3+}/Yb^{3+}/Er^{3+}$ glass is enhanced under direct excitation of Cr^{3+} at 600 nm. For $Cr^{3+}/Er^{3+}/Ho^{3+}$ glass, luminescence quenching of Er^{3+} and enhancement of Ho^{3+} at 2000 nm is quite well observed. Based on spectra and decays, the energy transfer processes $Cr^{3+} \rightarrow Yb^{3+} \rightarrow Er^{3+}$ and $Cr^{3+} \rightarrow Er^{3+} \rightarrow Ho^{3+}$ with their efficiencies equal to nearly 55% were identified. The presence of energy transfer processes was also confirmed using the excitation spectra measured under selective monitoring emission wavelengths. The results obtained for barium gallo-germanate glasses co-activated with $Cr^{3+}/Yb^{3+}/Er^{3+}$ and $Cr^{3+}/Er^{3+}/Ho^{3+}$ are promising for near-infrared luminescence applications.

Keywords Barium gallo-germanate glass, Cr^{3+} ions, Rare earth ions, Energy transfer process, Near-infrared luminescence

Rapid development in the fields of glass science and light technologies increased demand for rare earth doped amorphous systems emitting radiation in wide spectral range from UV-VIS to infrared as well as characterized by high resistance to crystallization and relatively large glass-forming region. Thus, thermally-stable rare earth activated glasses with promising physicochemical and optical properties belong to perspective materials exhibiting numerous applications in modern photonics. The past, present, and future of photonic glasses is reported in the excellent review published recently[1]. Systematic investigations revealed that many glass systems activated by trivalent rare earths are excellent candidates for solid-state lasers[2], whispering gallery mode micro-optical resonators[3], and full-color tuned volumetric displays achieved through the up-conversion luminescence process, offering wide range of potential applications in RGB technology[4,5]. In particular, rare earth co-doping expands significantly the application possibilities in glass photonics. Thanks to the excitation energy transfer processes and various radiative relaxation channels present in rare earth co-doped glasses, visible or infrared emission can be improved and tuned practically in broad spectral range. Among others, some inorganic glasses doubly[6–9] and triply[10–12] doped with rare earths are useful for VIS/NIR luminescence, blue up-conversion and white light generation. Especially, the impact of pair Er^{3+}/Yb^{3+} on near-infrared and mid-infrared emission at 1.5 and 2.7 μm, green and red up-conversion processes and optical temperature glass sensors have been examined in details[13–16]. Bismuth borosilicate glasses triply doped with $Ce^{3+}/Yb^{3+}/Er^{3+}$ are proposed as an excellent material for broadband fiber amplifiers, because near-infrared luminescence at 1.55 μm is enhanced (without sacrificing the lifetime) due to the phonon-assisted energy transfer (PAET) process between Er^{3+} and Ce^{3+} ions[17]. Enhancement of near-infrared luminescence at 2.05 μm in fluorotellurite glass triply doped with $Yb^{3+}/Er^{3+}/Ho^{3+}$ ions was obtained under 980 nm laser diode excitation[18].

Among some oxide systems, barium gallo-germanate glass referred as BGG is considered as one of the most important host matrices useful for multifunctional optical applications. Quite large glass-forming region and IR transmittance range combined with high thermal stability, rare earth solubility, relatively low phonon energy

[1]Institute of Chemistry, University of Silesia, Szkolna 9, Katowice 40-007, Poland. [2]Bialystok University of Technology, Wiejska 45D Street, Bialystok 15-351, Poland. [3]National Institute of Metrological Research (INRiM), Strada delle Cacce 91, Torino 10135, Italy. [4]AGH University of Krakow, 30 Mickiewicza Av, Krakow 30-059, Poland. ✉email: wojciech.pisarski@us.edu.pl

in comparison to other oxide glass systems and superior optical properties are the main advantages of BGG-type glasses. In 2011 germanate glass based on $BaO\text{-}Ga_2O_3\text{-}GeO_2$ composition was proposed as a window for high energy laser HEL systems[19]. BGG-type glasses singly doped[20–24] and co-doped[25–27] with rare earth ions are also recommended for near-infrared and mid-infrared laser sources. At this moment it worthy to notice that continuous-wave bulk laser around 2 μm in Tm^{3+}-doped BGG glass was demonstrated recently[28]. Also, femtosecond-laser-written single-scan waveguide was fabricated in Tm^{3+}-doped BGG glass and then lasing was successfully obtained[29]. Special attention has been paid to low-loss mid-infrared BGG fibers fabricated by Guerineau et al.[30–32] and BGG fibers co-doped with rare earths exhibiting ultrabroadband near-infrared emission at 1.5–2.1 μm[33–36]. The effect of Er^{3+}/Yb^{3+} content on the up-conversion process and infrared emission in BGG glass has been also analyzed under 980 nm excitation. Trivalent ytterbium is very good sensitizer in Yb^{3+}/Er^{3+} co-doped glass systems due to high absorption cross-section of Yb^{3+} ions at 980 nm (pumping of $^2F_{5/2}$ state) and spectral overlap between emission of donor ($^2F_{5/2} \rightarrow {}^2F_{7/2}$ transition of Yb^{3+}) and absorption of acceptor ($^4I_{15/2} \rightarrow {}^4I_{11/2}$ transition of Er^{3+}), leading to an efficient $Yb^{3+} \rightarrow Er^{3+}$ resonant energy transfer process. Xiao and Yang[25] suggest that Er^{3+}/Yb^{3+} co-doped barium gallo-germanate glasses are suitable for up-conversion and infrared luminescence applications and can be successfully used in fiber lasers and optical waveguide devices. BGG-type glasses co-doped with Er^{3+}/Yb^{3+} ions can be also applied to optical sensors[37]. Alternative to Yb^{3+} ions are transition metal ions (especially Cr^{3+}) with the spin-allowed transitions, which can be also widely used as a luminescent sensitizer for the parity-forbidden electronic transitions of rare earth ions. However, luminescence properties of barium gallo-germanate glasses and optical fibers containing transition metal and rare earth ions have been rarely studied[38].

Previous studies demonstrate that $Cr^{3+}/Yb^{3+}/Er^{3+}$ triply doped systems are really important for optical applications. In fact, reports on luminescence properties of inorganic phosphors and composite glass-ceramic composites triply doped with $Cr^{3+}/Yb^{3+}/Er^{3+}$ are mainly documented in literature. Some aspects for broadband Cr^{3+}-sensitized up-conversion luminescence in $La_3Ga_5GeO_{14}$ co-activated with $Cr^{3+}/Yb^{3+}/Er^{3+}$ have been presented and discussed in details[39]. Simultaneous near-infrared luminescence in I, II and III biological windows was realized through the energy transfer process in direction $Yb^{3+} \rightarrow Er^{3+}/Ho^{3+} \rightarrow Cr^{3+}$[40]. Simultaneously strong near-infrared luminescence (NIR-II/III windows) was also induced by $Cr^{3+}/Yb^{3+}/Er^{3+}$ energy transfer process present in $KScP_2O_7$[41]. These aspects have been studied for near-infrared thermometry, near-infrared pc-LED and night-vision applications. Down- and up-conversion luminescence processes have been also examined for $Cr^{3+}/Yb^{3+}/Er^{3+}$ ions in glass-ceramics containing crystalline phases[42–44]. Among others, down-conversion luminescence processes have been investigated for $Cr^{3+}/Yb^{3+}/Er^{3+}$ triply doped glass-ceramic composites with $\beta\text{-}PbF_2$ crystalline phase showing potential optical applications in the fields of full spectrum lighting and display[42]. Up-conversion luminescence processes and sensing properties have been analyzed for $Cr^{3+}/Yb^{3+}/Ln^{3+}$ (Ln = Er, Ho) triply doped glass-ceramics[43], where Cr^{3+} dopants were evidenced to be incorporated into the precipitated $LiGa_5O_8$ nanocrystals and Ln^{3+} ions remained in the precursor amorphous host. Also, $Cr^{3+}/Yb^{3+}/Er^{3+}$ triply doped LaF_3:Yb^{3+}/Er^{3+} and Ga_2O_3:Cr^{3+} dual-phase nanocrystals embedded into the aluminosilicate glass-ceramics have been studied for non-contact temperature sensors[44]. Contrary to these crystalline systems only a few works are devoted to $Cr^{3+}/Yb^{3+}/Er^{3+}$ triply doped glasses and their emission properties. Luminescence investigations were limited to phosphate and silicate glass systems. In 1990 $Cr^{3+}/Yb^{3+}/Er^{3+}$ triply doped fluoride phosphate glasses have been studied to explore their spectroscopic and laser properties[45]. Thirty years later, the influence of Cr^{3+} ions on yellowish-green up-conversion emission and energy transfer processes in zinc silicate glass triply doped with $Cr^{3+}/Yb^{3+}/Er^{3+}$ has been also analyzed in details[46]. To the best of our knowledge, emission properties of $Cr^{3+}/Yb^{3+}/Er^{3+}$ ions in barium gallo-germanate glass have not been yet studied.

The introduction of chromium ions into Ln^{3+}- doped glass has several advantages. One of them is related to strong and broad absorption bands of transition metal ions necessary to efficient pumping of the glass host. However, co-doping Cr^{3+} and Ln^{3+} ions in glasses leads also to some limitations. Owing to high activator (Cr^{3+} and Ln^{3+}) concentrations and their low solubility in some glasses, the mutual interactions between transition metal and/or rare earth ions can give important contribution to clustering effects and cross-relaxation processes. Consequently, non-radiative relaxation channels start to dominate in such glass systems. For that reason, the relatively low activator concentrations are strongly recommended for Cr^{3+}/Ln^{3+} co-doped glass systems. When the energy transfer process is efficient and the energy matching between excites states of transition metal and rare earths is very well, the back energy transfer processes are often present in some glass systems (especially low-phonon glasses) resulted in depopulation of the upper laser states. Generally, all processes mentioned above may lead to luminescence quenching in Cr^{3+}/Ln^{3+} co-doped glass systems, which have been rarely reported in literature. These aspects motivated us to undertake research on inorganic glasses doubly and triply doped with transition metal and rare earth ions emitting near-infrared radiation.

The intension of current work is to investigate near-infrared luminescence properties of barium gallo-germanate glasses co-doped with Cr^{3+}/Er^{3+} in the absence and presence of Yb^{3+} or Ho^{3+}. Our previous investigations for Cr^{3+} doped BGG glass shown that chromium ions are located in an intermediate octahedral ligand field surrounding (Dq/B = 2.13 from the Tanabe-Sugano diagram) and occur in the trivalent oxidation state (EPR signals at g = 4.8 and g = 1.97), which was evidenced by the electron paramagnetic resonance and optical absorption spectroscopy[47]. The concentration-dependent luminescence properties have been also examined and the molar concentrations of activators in BGG glasses doubly doped with Cr^{3+} and Ho^{3+} were optimized. The studies concerning on Cr^{3+}/Ho^{3+} co-doped BGG glass emitting near-IR radiation revealed that the integrated intensities of emission bands are maximal at 0.25 mol% Cr^{3+}/0.5 mol% Ho^{3+} ref[48]. Very recently, it was also found that BGG-type glasses are promising inorganic materials for near-IR emission applications after $Cr^{3+}/Tm^{3+}/Ho^{3+}$ triple doping[49].

Here, near-infrared luminescence properties of barium gallo-germanate glasses co-activated with Cr^{3+}/Er^{3+} and $Cr^{3+}/Er^{3+}/Ln^{3+}$ (Ln = Yb, Ho) are presented and discussed. Near-infrared luminescence corresponding to

$^4I_{13/2} \rightarrow {}^4I_{15/2}$ transition of Er^{3+} ions was detected under direct excitation of Cr^{3+} and its emission intensity is enhanced significantly in $Cr^{3+}/Yb^{3+}/Er^{3+}$ triply doped BGG glass compared to Cr^{3+}/Er^{3+} doubly doped sample. The energy transfer processes in direction $Cr^{3+} \rightarrow Er^{3+}$ and $Cr^{3+} \rightarrow Yb^{3+} \rightarrow Er^{3+}$ occur. Completely different situation is observed for $Cr^{3+}/Er^{3+}/Ho^{3+}$ triply doped BGG glass, where near-infrared emission of erbium at 1.5 µm is reduced due to presence of energy transfer from Er^{3+} to Ho^{3+} ions. The following energy transfer processes $Cr^{3+} \rightarrow Ln^{3+}$ (Ln = Er and Ho) and $Cr^{3+} \rightarrow Er^{3+} \rightarrow Ho^{3+}$ are well evidenced. The energy transfer efficiencies were determined based on the emission decay curve analysis. The presence of the energy transfer processes was also confirmed by the excitation spectra measurements. The experimental results evidently suggest that both $Cr^{3+}/Yb^{3+}/Er^{3+}$ and $Cr^{3+}/Er^{3+}/Ho^{3+}$ co-activated barium gallo-germanate glasses belong to promising near-infrared emitting glass systems under direct excitation of Cr^{3+} ions at 600 nm.

Results and discussion

Barium gallo-germanate glasses co-activated with Cr^{3+}/Er^{3+} and $Cr^{3+}/Er^{3+}/Ln^{3+}$ ions (where Ln = Yb, Ho) were synthetized by high temperature melt quenching method and their chemical compositions are given in Table 1. Optical properties of the studied systems were also compared to the results obtained for BGG glass samples singly doped with Cr^{3+} and doubly doped with Cr^{3+}/Yb^{3+} and Cr^{3+}/Ho^{3+} ions. Additionally, BGG glass sample singly doped with Eu^{3+} (0.5Eu) was prepared in order to obtain the phonon energy from the excitation spectrum measurement.

In the first step, BGG glass-host was characterized using DSC method in order to determine characteristic temperatures and thermal stability. Also, phonon energy was evaluated using the Raman spectrum and Eu^{3+} excitation spectrum measurement. The results are given in Fig. 1.

Thermal investigations indicated that DSC curves for BGG glass samples doubly or triply doped with Cr^{3+} and Ln^{3+} are nearly unchanged, because molar concentrations of activators are relatively low. Based on DSC curve measured for the representative BGG sample, characteristic temperatures such as the glass transition temperature (T_g), the crystallization onset (T_x) and the maximum of the crystallization peak (T_p) were determined. The characteristic temperatures for BGG glass sample are as follows: T_g = 620 °C, T_x = 805 °C and T_p = 844 °C. The thermal stability parameter referred as $\Delta T = T_x - T_g$ is relatively large and its value is close to 185 °C, which suggest that BGG glass system is promising to optical fiber drawing.

The excitation spectrum measured for Eu^{3+}-doped BGG glass under the monitoring emission wavelength 610 nm ($^5D_0 \rightarrow {}^7F_2$ red luminescent transition of Eu^{3+}) shows several bands due to transitions originating from the $^7F_0$ ground state to the higher-lying excited states, respectively. Two of them, $^7F_0 \rightarrow {}^5D_1$ and $^7F_0 \rightarrow {}^5D_2$ transitions of Eu^{3+} are presented in Fig. 1. The later transition, i.e. the $^7F_0 \rightarrow {}^5D_2$ transition is known as pure electronic transition (PET), which is associated with the phonon sideband (PSB) situated in this spectral range. The phonon energy of the glass host can be quite easily estimated from the difference between the positions of both PSB and PET bands. For BGG glass system, PSB – PET is equal to 790 cm^{-1} and its value quite well corresponds with the results obtained from the Raman spectrum measurement shown in the inset of Fig. 1.

In order to characterize BGG glasses co-doped with Cr^{3+}/Er^{3+} the X-ray diffraction patterns and VIS-NIR optical absorption spectra were measured. They are presented on Fig. 2.

The XRD patterns for Cr^{3+}/Er^{3+} co-doped BGG samples are typical for amorphous systems and no narrow diffraction lines due to crystalline phase was detected. It suggests that BGG type glasses are able to accommodate transition metal and rare earth ions and they are still fully amorphous.

Visible absorption spectra measured for Cr^{3+}/Er^{3+} co-doped BGG glass samples consist of broad and narrow bands characteristic for transition metal and rare earths. Broad spin-allowed absorption band at about 600 nm is assigned to $^4A_2 \rightarrow {}^4T_2$ transition of trivalent Cr^{3+} ions. Interestingly, narrow absorption peak near 700 nm (well known as R-line) corresponding to spin-forbidden $^2E \rightarrow {}^4T_2$ transition of Cr^{3+} is also quite well observed. Broad band of Cr^{3+} ions is overlapped with narrow absorption line situated at about 650 nm, which corresponds to the $^4I_{15/2} \rightarrow {}^4F_{9/2}$ transition of Er^{3+}. Other lines due to transitions originating from the $^4I_{15/2}$ ground state to the higher-lying $^4S_{3/2}$, $^2H_{11/2}$ and $^4F_{7/2}$ excited states of Er^{3+} ions are located on the absorption edge. In the infrared spectral range, two characteristic absorption bands at 980 nm and 1500 nm related to $^4I_{15/2} \rightarrow {}^4I_{11/2}$ and $^4I_{15/2} \rightarrow {}^4I_{13/2}$ transition of Er^{3+} ions were identified. The intensities of absorption bands increase with increasing Er^{3+} ion concentration.

Glass code	Chemical composition [mol%]
0.5Eu	$60GeO_2$–30BaO-9.5Ga_2O_3–0.5Eu_2O_3
0.25Cr	$60GeO_2$–30BaO-9.75Ga_2O_3–0.25Cr_2O_3
0.25Cr-0.5Yb	$60GeO_2$–30BaO-9.25Ga_2O_3–0.25Cr_2O_3–0.5Yb_2O_3
0.25Cr-0.5Ho	$60GeO_2$–30BaO-9.25Ga_2O_3–0.25Cr_2O_3–0.5Ho_2O_3
0.25Cr-0.1Er	$60GeO_2$–30BaO-9.65Ga_2O_3–0.25Cr_2O_3–0.1Er_2O_3
0.25Cr-0.5Er	$60GeO_2$–30BaO-9.25Ga_2O_3–0.25Cr_2O_3–0.5Er_2O_3
0.25Cr-1.0Er	$60GeO_2$–30BaO-8.75Ga_2O_3–0.25Cr_2O_3–1.0Er_2O_3
0.25Cr-0.5Yb-0.5Er	$60GeO_2$–30BaO-8.75Ga_2O_3–0.25Cr_2O_3–0.5Yb_2O_3-0.5Er_2O_3
0.25Cr-0.5Er-0.5Ho	$60GeO_2$–30BaO-8.75Ga_2O_3–0.25Cr_2O_3–0.5Er_2O_3-0.5Ho_2O_3

Table 1. Chemical composition of BGG glasses.

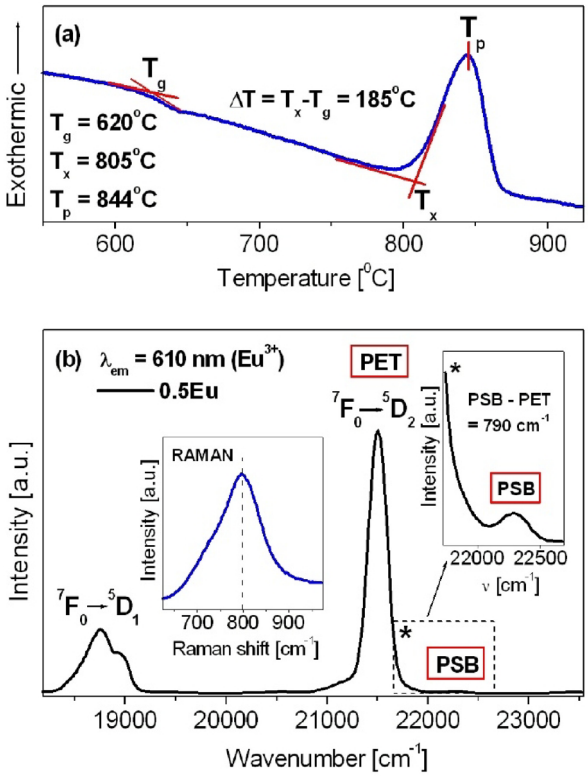


Fig. 1. (**a**) DSC curve for the representative glass sample and (**b**) the excitation spectrum of BGG glass singly doped with Eu^{3+}. The Raman spectrum is also shown in the inset.

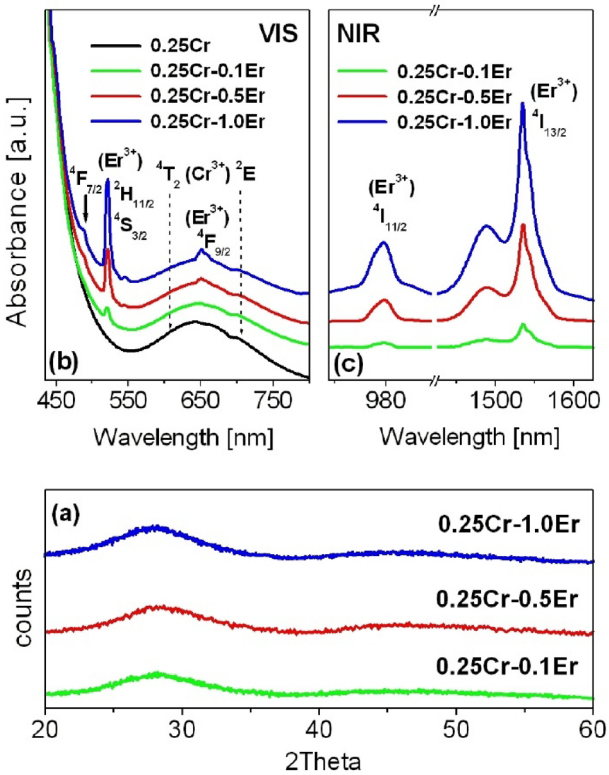


Fig. 2. (**a**) X-ray diffraction patterns and absorption spectra of BGG glasses co-doped with Cr^{3+}/Er^{3+} measured in (**b**) visible and (**c**) near-infrared ranges.

Figure 3 presents near-infrared emission spectra of BGG glasses co-doped with Cr^{3+}/Er^{3+}. The spectra were measured under direct excitation of Cr^{3+} at 600 nm and Er^{3+} at 980 nm. The most intense near-infrared emission band centered at 1534 nm corresponds to $^4I_{13/2} \rightarrow {}^4I_{15/2}$ laser transition of Er^{3+} ions, which is important for optical amplification[50–54]. Additionally, low-intensity emission band near 1100 nm associated with $^4T_2 \rightarrow {}^4A_2$ transition of chromium ions is observed for Cr^{3+}/Er^{3+} co-doped BGG glasses excited directly at 600 nm (Cr^{3+}). Especially, it is well evidenced for 0.25Cr-0.1Er glass sample. Independently on the excitation wavelength 600 nm (Cr^{3+}) or 980 nm (Er^{3+}), the intensity of emission band related to $^4I_{13/2} \rightarrow {}^4I_{15/2}$ transition of Er^{3+} is the highest for 0.25Cr-0.5Er glass. Similar situation was also observed for Cr^{3+}/Ho^{3+} co-doped BGG glass system[48], where the integrated intensity of emission band at 2000 nm due to $^5I_7 \rightarrow {}^5I_8$ transition of Ho^{3+} is found to be maximal for 0.25Cr-0.5Ho glass sample. However, the most important information is that near-infrared luminescence of erbium ions in Cr^{3+}/Er^{3+} co-doped BGG glass is observed under direct excitation of Cr^{3+} ions at 600 nm, suggesting the presence of the energy transfer process $Cr^{3+} \rightarrow Er^{3+}$. These observations are also consistent with the experimental results obtained for Cr^{3+}/Er^{3+} ions in TeO_2-$PbCl_2$ tellurite glass, where the efficient energy transfer in direction from Cr^{3+} to Er^{3+} occurs[55]. The presence of the energy transfer process between Cr^{3+} and Er^{3+} ions was confirmed by the emission decay curve measurements. Luminescence decay curves for BGG glasses co-doped with Cr^{3+}/Er^{3+} ions were measured under 600 nm excitation and monitoring emission wavelength 1070 nm. The results are compared to BGG glass sample singly doped with Cr^{3+}. Based on decay curves, the energy transfer efficiency η_{ET} (given in %) was calculated using the following relation:

$$\eta_{ET} = 1 - \frac{\tau_{Cr-Er}}{\tau_{Cr}} \quad (1)$$

where τ_{Cr-Er} and τ_{Cr} are luminescence lifetimes for the $^4T_2$ state of Cr^{3+} ions in glass samples with the presence and absence of acceptor (Er^{3+}) ions.

Decay curves for the $^4T_2$ (Cr^{3+}) state in BGG glasses containing Cr^{3+} and Cr^{3+}/Er^{3+} ions are shown in Fig. 4. Lifetimes and energy transfer efficiencies are also schematically illustrated.

The measurements for Cr^{3+}/Er^{3+} co-doped BGG glasses indicate that luminescence decay curves are shorter compared to glass sample without Er^{3+} ions, suggesting the efficient energy transfer process from donor (Cr^{3+}) to acceptor (Er^{3+}) ions. Luminescence lifetime measured for the $^4T_2$ state in Cr^{3+} singly doped BGG glass (0.25Cr) is close to 14.15 µs and its experimental value is reduced to 9.35 µs (0.25Cr-0.1Er), 6.9 µs (0.25Cr-0.5Er) and 5.35 µs (0.25Cr-1.0Er) for glass samples with the presence of Er^{3+} ions. Thus, the energy transfer efficiencies increase from 34% (0.25Cr-0.1Er) up to 51% (0.25Cr-0.5Er) and 62% (0.25Cr-1.0Er), respectively. Compared to 0.25Cr-

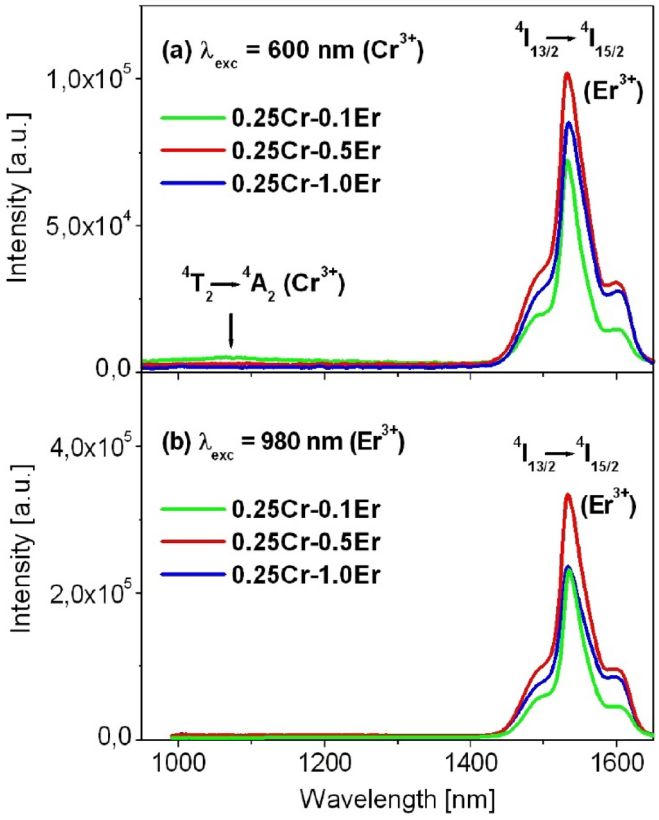


Fig. 3. Near-infrared luminescence spectra of BGG glasses co-doped with Cr^{3+}/Er^{3+} measured under direct excitation of (**a**) Cr^{3+} ions at 600 nm and (**b**) Er^{3+} ions at 980 nm.

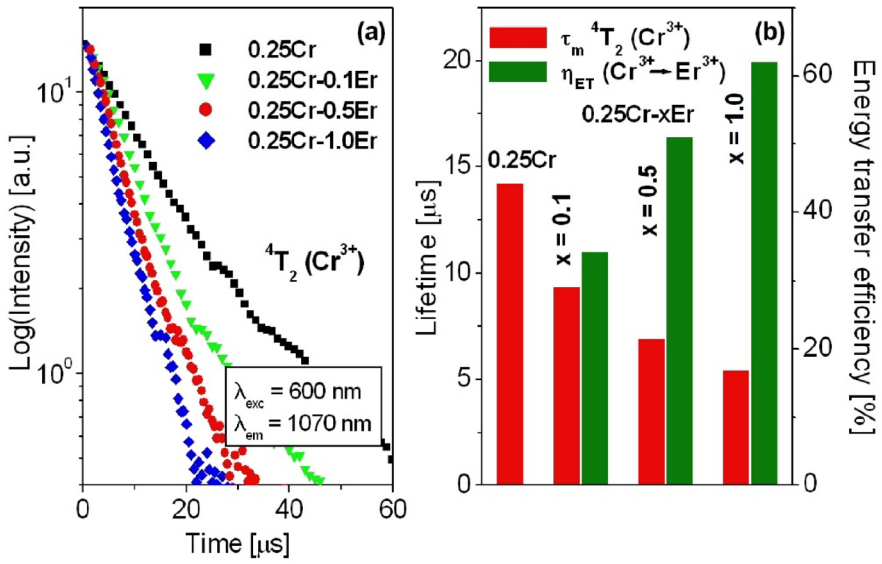


Fig. 4. (**a**) Luminescence decays from the^4 T_2 state of chromium in BGG glasses singly doped with Cr^{3+} ions and co-doped with Cr^{3+}/Er^{3+} ions. (**b**) Lifetimes and energy transfer efficiencies are also schematically illustrated.

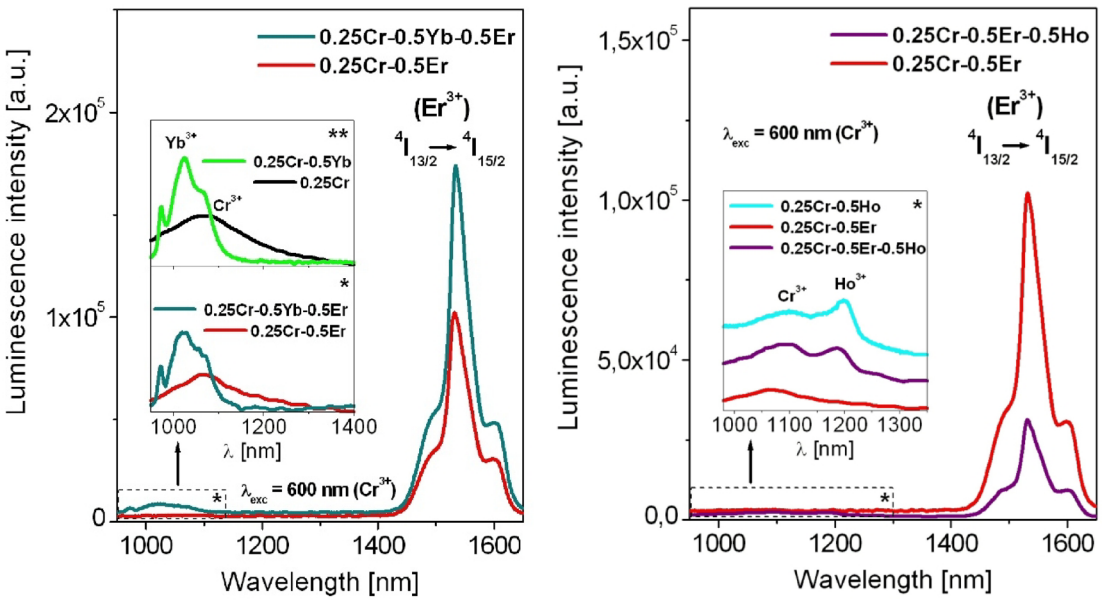


Fig. 5. Near-infrared luminescence spectra of BGG glasses doubly doped with Cr^{3+}/Er^{3+} ions and triply doped with $Cr^{3+}/Yb^{3+}/Er^{3+}$ and $Cr^{3+}/Er^{3+}/Ho^{3+}$ ions measured under direct excitation of Cr^{3+} at 600 nm. The insets show (*) normalized emission spectra for the studied glasses in 950–1400 nm range compared to glass samples singly doped with Cr^{3+} ions and co-doped with Cr^{3+}/Yb^{3+} and Cr^{3+}/Ho^{3+} ions.

1.0Ho glass sample with $\tau = 10.9$ μs and $\eta_{ET} = 23\%$[48] we suggest that the energy transfer process is more efficient for BGG glass co-doped with Cr^{3+}/Er^{3+} than Cr^{3+}/Ho^{3+}.

In the next step, near-infrared luminescence properties of Cr^{3+}/Er^{3+} co-doped BGG glasses with the absence and presence of Yb^{3+} or Ho^{3+} ions are compared. Near-infrared luminescence spectra for BGG glasses doubly doped with Cr^{3+}/Er^{3+} (0.25Cr-0.5Er) and triply doped with $Cr^{3+}/Yb^{3+}/Er^{3+}$ (0.25Cr-0.5Yb-0.5Er) and $Cr^{3+}/Er^{3+}/Ho^{3+}$ (0.25Cr-0.5Er-0.5Ho) were measured under direct excitation of Cr^{3+} ions at 600 nm. The results are presented in Fig. 5.

The insets of Fig. 5 denoted as (*) show normalized near-infrared luminescence spectra measured in 950–1400 nm range for BGG glasses co-activated with Cr^{3+}/Er^{3+} and $Cr^{3+}/Er^{3+}/Ln^{3+}$ (Ln = Yb or Ho). The results are compared to glass samples singly doped with Cr^{3+} ions and co-doped with Cr^{3+}/Yb^{3+} and Cr^{3+}/Ho^{3+}. For

0.25Cr-0.5Er glass sample, emission band centered at 1100 nm corresponds to $^4T_2 \rightarrow {}^4A_2$ transition of Cr^{3+} ions. The profile of emission band is comparable to that one obtained for Cr^{3+}-singly doped glass. Compared to Cr^{3+}/Yb^{3+} co-doped sample (**), the spectrum measured for 0.25Cr-0.5Yb-0.5Er glass consists of two overlapped emission bands related to $^4T_2 \rightarrow {}^4A_2$ (Cr^{3+}) and $^2F_{5/2} \rightarrow {}^2F_{7/2}$ (Yb^{3+}) transitions. Analogously, two emission bands near 1100 nm and 1200 nm are quite well visible for 0.25Cr-0.5Er-0.5Ho glass, which was compared to Cr^{3+}/Ho^{3+} co-doped glass sample. Near-infrared luminescence bands are assigned to $^4T_2 \rightarrow {}^4A_2$ (Cr^{3+}) and $^5I_6 \rightarrow {}^5I_8$ (Ho^{3+}) transitions, respectively. However, the most important information is that the integrated intensity of luminescence band due to main $^4I_{13/2} \rightarrow {}^4I_{15/2}$ laser transition of Er^{3+} at 1534 nm is changed drastically for Cr^{3+}/Er^{3+} co-doped BGG glasses with the presence of Yb^{3+} and Ho^{3+}. The changes in luminescence intensities are completely different for glass sample with $Cr^{3+}/Yb^{3+}/Er^{3+}$ than $Cr^{3+}/Er^{3+}/Ho^{3+}$. Near-infrared luminescence in 0.25Cr-0.5Er-0.5Ho glass is reduced significantly (3.4-fold decrease), whereas 1.6-fold emission enhancement is observed for 0.25Cr-0.5Yb-0.5Er glass. Emission linewidth defined as full width at half maximum (FWHM) decreases slightly from 48 nm (0.25Cr-0.5Er) to 43 nm (0.25Cr-0.5Yb-0.5Er) and 45.5 nm (0.25Cr-0.5Er-0.5Ho), respectively. Based on the emission spectra measurements we suggest that different mechanisms are responsible for the enhancement/quenching near-infrared luminescence of Er^{3+} at 1534 nm in Cr^{3+}/Er^{3+} co-doped glass samples with the presence of Yb^{3+} and Ho^{3+} under direct excitation of Cr^{3+} at 600 nm. The mechanisms for BGG glasses triply doped with $Cr^{3+}/Yb^{3+}/Er^{3+}$ and $Cr^{3+}/Er^{3+}/Ho^{3+}$ ions involving radiative/nonradiative relaxation channels and possible energy transfer, i.e. energy transfer routes (ET), multiphonon relaxation (MPR) and luminescent transitions of Cr^{3+} and Ln^{3+} ions are illustrated on the energy level diagrams, which are shown in Fig. 6.

When glass sample co-activated with $Cr^{3+}/Er^{3+}/Ln^{3+}$ ions (Ln = Yb, Ho) is directly pumped at 600 nm, part of the excitation energy is transferred from Cr^{3+} to Er^{3+} (ET1). The excitation energy transfers nonradiatively to the lower-lying states by multiphonon relaxation (MPR) and then relaxes radiatively from the upper $^4I_{13/2}$ laser state of Er^{3+} ions generating near-infrared emission at 1534 nm. Consequently, we can observe low-intensity and high-intensity emission bands corresponding to $^4T_2 \rightarrow {}^4A_2$ (Cr^{3+}) and $^4I_{13/2} \rightarrow {}^4I_{15/2}$ (Er^{3+}) transitions. For $Cr^{3+}/Yb^{3+}/Er^{3+}$ co-activated glass system, part of the excitation energy is also transferred by ET2 and ET3 processes from Cr^{3+} to Er^{3+} via Yb^{3+} ions playing the bridging role. Thus, we can also observe low-intensity emission band associated with $^2F_{5/2} \rightarrow {}^2F_{7/2}$ transition of Yb^{3+} ions. In this case, the energy transfer process $Cr^{3+} \rightarrow Yb^{3+} \rightarrow Er^{3+}$ is quite efficient and near-infrared emission of Er^{3+} ions at 1534 nm is enhanced greatly in comparison to Cr^{3+}/Er^{3+} co-doped glass sample. Similar pathway $Nd^{3+} \rightarrow Yb^{3+} \rightarrow Er^{3+}$ was also proposed earlier for $Nd^{3+}/Yb^{3+}/Er^{3+}$ triply doped Ba-Al-metaphosphate glasses, where the Yb^{3+} ions are found to be providing efficient bridging action for the energy transfer process from Nd^{3+} to Er^{3+} ions and near-infrared luminescence sensitization[56].

For BGG glass co-activated with $Cr^{3+}/Er^{3+}/Ho^{3+}$ ions, part of the excitation energy is also transferred from Cr^{3+} to Ho^{3+} (ET2). Then, the energy relaxes nonradiatively by MPR processes to the lower-lying $5I_6$ and $5I_7$ excited states, from which near-infrared luminescent transitions to the $5I_8$ ground state of Ho^{3+} occur. It was also confirmed by us for BGG glasses doubly doped with Cr^{3+}/Ho^{3+} ions[48]. Among others, it resulted in an efficient

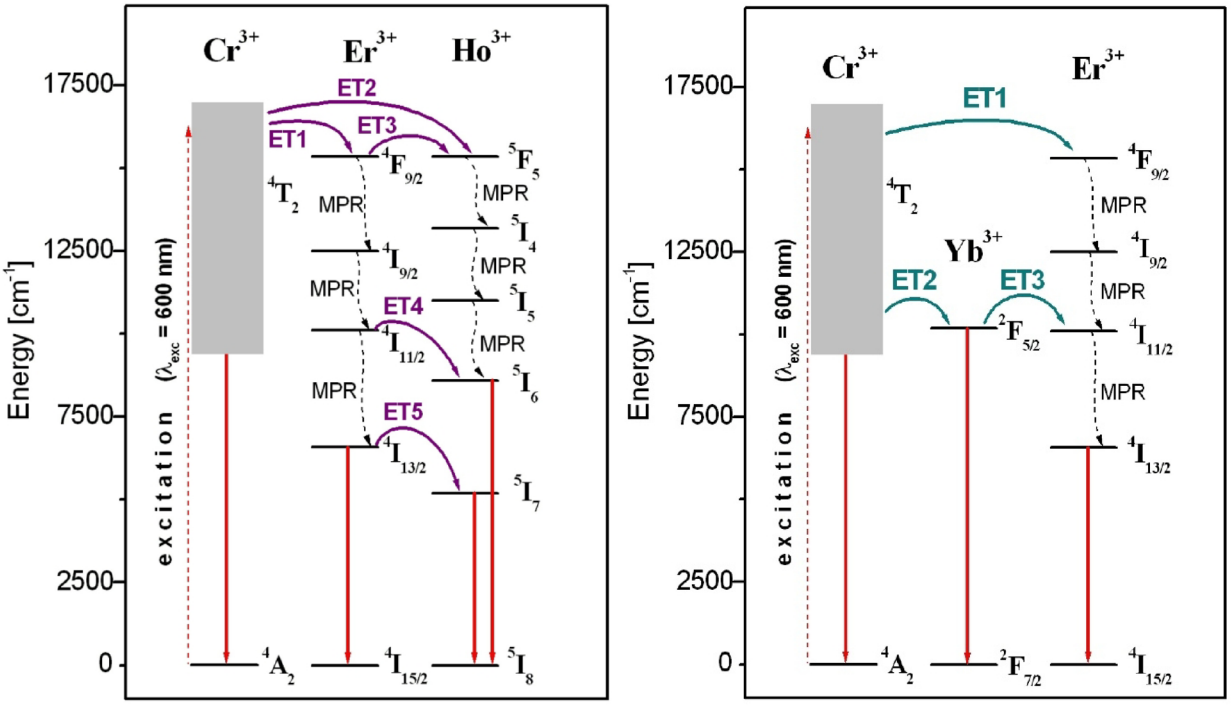


Fig. 6. Energy level diagram for BGG glass co-doped with $Cr^{3+}/Yb^{3+}/Er^{3+}$ and $Cr^{3+}/Er^{3+}/Ho^{3+}$. All transitions and energy transfer processes are also indicated for glass samples excited directly at 600 nm (Cr^{3+}).

near-infrared emission at 2 μm due to $^5I_7 \rightarrow {}^5I_8$ transition of Ho^{3+} in fluorogermanate glass, which was sensitized by Cr^{3+} ions[57]. At this moment, it should be also pointed that the Er^{3+} and Ho^{3+} ions interact with each other. Previous studies revealed that the following excitation energy transfer processes ET3, ET4 and ET5 (Fig. 5) are present in BGG glasses[26] and other glass systems[58,59–60] co-doped with Er^{3+}/Ho^{3+}: $^4F_{9/2}$ (Er^{3+}) → $^5F_5$ (Ho^{3+}), $^4I_{11/2}$ (Er^{3+}) → $^5I_6$ (Ho^{3+}) and $^4I_{13/2}$ (Er^{3+}) → $^5I_7$ (Ho^{3+}). In particular, the results for germanosilicate glasses co-doped with Er^{3+}/Ho^{3+} indicated that the dominant energy transfer process is $^4I_{13/2}$ (Er^{3+}) → $^5I_7$ (Ho^{3+}) than $^4I_{11/2}$ (Er^{3+}) → $^5I_6$ (Ho^{3+}) giving important contribution to near-infrared luminescence of Ho^{3+} ions at 2 μm[60]. The presence of near-infrared luminescent lines of Er^{3+} and Ho^{3+} ions at 1534 nm and 2000 nm in BGG glasses co-activated with $Cr^{3+}/Er^{3+}/Ln^{3+}$ (Ln = Yb or Ho) is due to efficient energy transfer processes $Cr^{3+} \rightarrow Yb^{3+} \rightarrow Er^{3+}$ and $Cr^{3+} \rightarrow Er^{3+} \rightarrow Ho^{3+}$ under direct excitation of Cr^{3+} ions at 600 nm. Luminescence decay curve analysis for BGG glasses triply doped with $Cr^{3+}/Er^{3+}/Ln^{3+}$ ions (where Ln = Yb, Ho) confirms this hypothesis.

Similar to Cr^{3+}/Er^{3+} co-doped glass samples, luminescence decay curve for BGG glass with $Cr^{3+}/Er^{3+}/Ho^{3+}$ was measured under direct excitation of Cr^{3+} ions at 600 nm and compared to samples singly doped with Cr^{3+} ions and co-doped with Cr^{3+}/Ln^{3+} (Ln = Er, Ho). The results are shown in Fig. 7. Lifetimes and energy transfer efficiencies are also schematically illustrated.

The experimental luminescence lifetime $4T_2$ (Cr^{3+}) has decreased from 14.15 μs (0.25Cr) to 12.4 μs (0.25Cr-0.5Ho), 6.9 μs (0.25Cr-0.5Er) and 6.2 μs (0.25Cr-0.5Er-0.5Ho), Accordingly, the energy transfer efficiencies $Cr^{3+} \rightarrow Ln^{3+}$ are found to be 12.4% (0.25Cr-0.5Ho), 51% (0.25Cr-0.5Er) and 56% (0.25Cr-0.5Er-0.5Ho), respectively. Decay curves analysis shown that the energy transfer process is more efficient for $Cr^{3+} \rightarrow Er^{3+}$ ($\eta_{ET} = 51\%$) than $Cr^{3+} \rightarrow Ho^{3+}$ ($\eta_{ET} = 12.4\%$). Similar phenomena are also observed for samples exhibiting the energy transfer $Cr^{3+} \rightarrow Er^{3+}$ and $Cr^{3+} \rightarrow Yb^{3+}$. The energy transfer efficiency is higher for glass co-doped with Cr^{3+}/Er^{3+} than Cr^{3+}/Yb^{3+}. For BGG glasses co-activated with Cr^{3+}/Ln^{3+} (Ln = Yb, Er) and $Cr^{3+}/Yb^{3+}/Er^{3+}$, the luminescence lifetimes $4T_2$ (Cr^{3+}) are reduced from 14.15 μs (0.25Cr) up to 11.6 μs (0.25Cr-0.5Yb), 6.9 μs (0.25Cr-0.5Er) and 6.5 μs (0.25Cr-0.5Yb-0.5Er), whereas the energy transfer efficiencies are changed from 18% (0.25Cr-0.5Yb) to 51% (0.25Cr-0.5Er) and 54% (0.25Cr-0.5Yb-0.5Er). The results from decay curve measurements are shown in Fig. 8.

Compared to Cr^{3+}/Ln^{3+} co-doped glass samples the measured lifetime is reduced, whereas the energy transfer efficiency increases for BGG glass systems triply doped with $Cr^{3+}/Er^{3+}/Ho^{3+}$ and $Cr^{3+}/Yb^{3+}/Er^{3+}$ suggesting the presence of additional interactions between Er^{3+} and Ho^{3+} ions as well as Yb^{3+} and Er^{3+} ions. It should be also emphasized that the decay curve analysis is more complicated for BGG glasses co-activated with Cr^{3+}/Yb^{3+} and $Cr^{3+}/Yb^{3+}/Er^{3+}$ ions. Luminescence decay curves were measured under the same experimental conditions, i.e. direct excitation of Cr^{3+} ions at 600 nm and monitoring emission wavelength 1070 nm. Decay curves are biexponential with short-lived and long-lived components. The short-lived components for both samples with Cr^{3+}/Yb^{3+} and $Cr^{3+}/Yb^{3+}/Er^{3+}$ correspond to luminescence decay of Cr^{3+} ions. Luminescence decay is shorter and the energy transfer efficiency is higher for glass sample triply doped with $Cr^{3+}/Yb^{3+}/Er^{3+}$. The long-lived components for BGG glasses co-doped with Cr^{3+}/Yb^{3+} and $Cr^{3+}/Yb^{3+}/Er^{3+}$ ions are completely different and their experimental values are in a good agreement with the results from decay curve measurements performed under direct excitation of Yb^{3+} at 940 nm and monitoring emission wavelength 1020 nm. The experiments clearly demonstrated that long-lived component is related to emission decay from $^2F_{5/2}$ state of Yb^{3+}. Compared

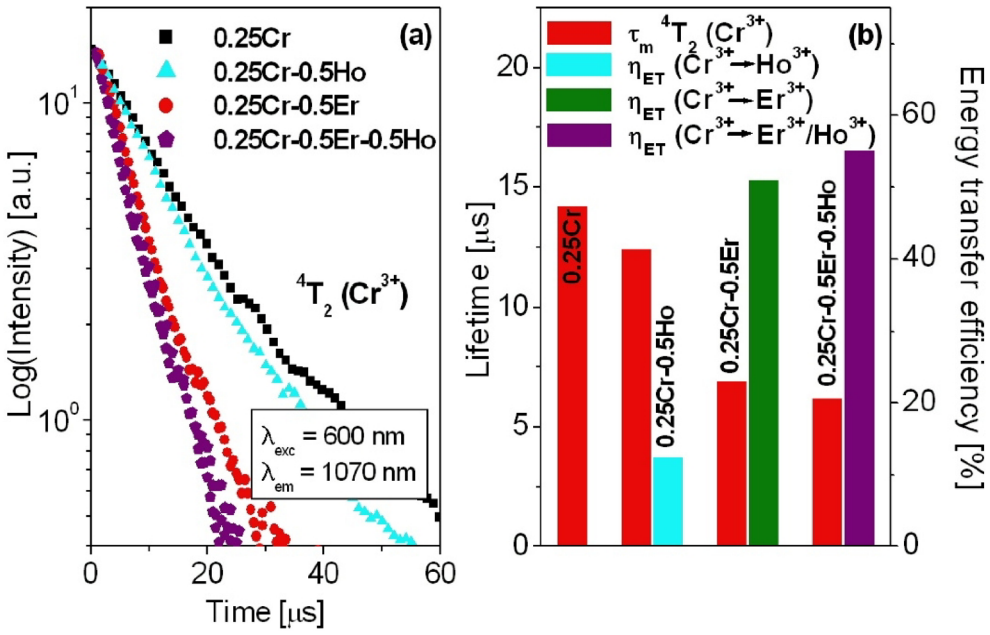


Fig. 7. (**a**) Luminescence decays for BGG glasses co-doped with Cr^{3+}/Ln^{3+} (Ln = Er, Ho) and $Cr^{3+}/Er^{3+}/Ho^{3+}$ measured under direct excitation of Cr^{3+} ions at 600 nm. (**b**) Lifetimes and energy transfer efficiencies are also schematically illustrated.

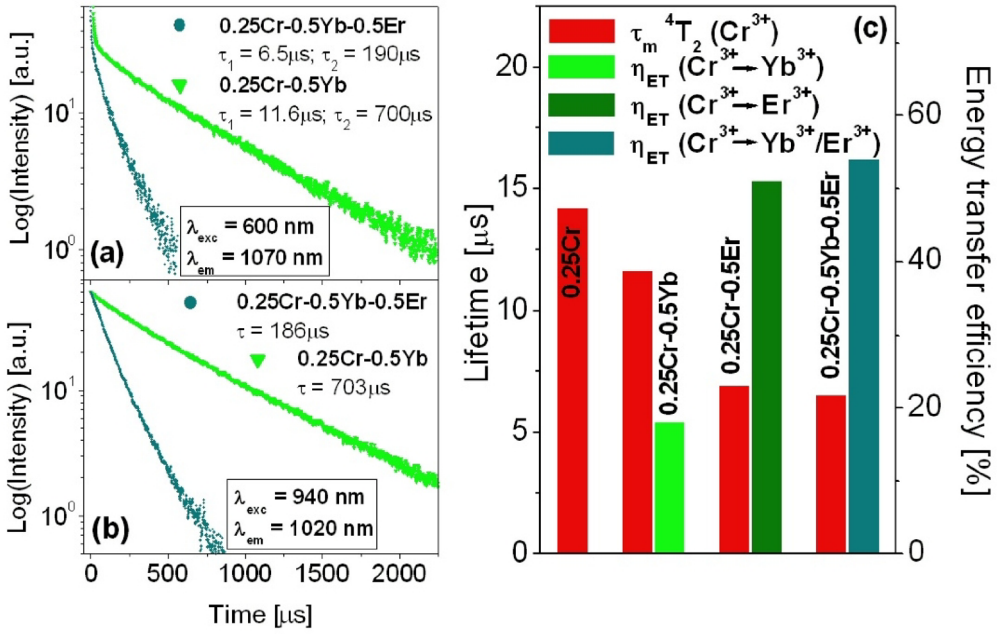


Fig. 8. Luminescence decays for BGG glasses co-doped with Cr^{3+}/Yb^{3+} and $Cr^{3+}/Yb^{3+}/Er^{3+}$ measured under direct excitation of (**a**) Cr^{3+} at 600 nm and (**b**) Yb^{3+} at 940 nm. (**c**) Lifetimes and energy transfer efficiencies are also schematically illustrated.

to Cr^{3+}/Yb^{3+} co-doped glass sample, the long-lived component is reduced significantly for BGG glass with the presence of Er^{3+} ions. Its value decreases from 700 μs (0.25Cr-0.5Yb) to nearly 190 μs (0.25Cr-0.5Yb-0.5Er). It suggests that the efficient energy transfer process $Yb^{3+} \rightarrow Er^{3+}$ is present in $Cr^{3+}/Yb^{3+}/Er^{3+}$ triply doped BGG glass excited directly at 600 nm (Cr^{3+}). Further decay curve measurements for BGG glasses co-activated with $Cr^{3+}/Er^{3+}/Ln^{3+}$ (Ln = Yb, Ho) under direct excitation of Cr^{3+} at 600 nm and monitoring emission wavelength 1534 nm (Er^{3+}) confirmed the presence of energy transfer processes $Yb^{3+} \rightarrow Er^{3+}$ and $Er^{3+} \rightarrow Ho^{3+}$.

Figure 9 shows luminescence decays from the $^4I_{13/2}$ excited states of Er^{3+} ions in BGG glasses doubly doped with Cr^{3+}/Er^{3+} and triply doped with $Cr^{3+}/Yb^{3+}/Er^{3+}$ and $Cr^{3+}/Yb^{3+}/Er^{3+}$ ions. Also, luminescence lifetimes are shown schematically in the inset. Luminescence lifetimes for the $^4I_{13/2}$ state of Er^{3+} in BGG glasses with Cr^{3+} and Ln^{3+} ions are close to 5.3 ms (0.25Cr-0.5Er), 2.8 ms (0.25Cr-0.5Er-0.5Ho) and 6.2 ms (0.25Cr-0.5Yb-0.5Er). It evidently suggests that the measured lifetime $^4I_{13/2}$ (Er^{3+}) is reduced for Cr^{3+}/Er^{3+} co-doped BGG glass with the presence of Ho^{3+} and increases for glass sample with the presence of Yb^{3+}. Also, decay curve measured for 0.25Cr-0.5Yb-0.5Er glass exhibits a clear rise time (*) followed by a luminescence decay from the $^4I_{13/2}$ state of Er^{3+} ions, which is also shown in the inset of Fig. 9. These effects are not observed for 0.25Cr-0.5Er and 0.25Cr-0.5Er-0.5Ho glass systems.

The presence of a rise time together with longer emission lifetime $^4I_{13/2}$ (Er^{3+}) compared to 0.25Cr-0.5Er co-doped sample provide strong evidence that the near-infrared luminescence at 1534 nm in BGG glass excited directly at 600 nm (Cr^{3+}) occurs through an efficient energy transfer from Cr^{3+} via Yb^{3+} to Er^{3+} ions. Reduction of measured lifetime for $^2F_{5/2}$ state of Yb^{3+} (long-lived component, see Fig. 8) from 700 μs (0.25Cr-0.5Yb) to 190 μs (0.25Cr-0.5Yb-0.5Er) and the increase in luminescence lifetime for the $^4I_{13/2}$ state of Er^{3+} from 5.3 ms (0.25Cr-0.5Er) to 6.2 ms (0.25Cr-0.5Yb-0.5Er) is the experimental proof of the energy transfer process $Yb^{3+} \rightarrow Er^{3+}$ present in BGG glass triply doped with $Cr^{3+}/Yb^{3+}/Er^{3+}$ under direct excitation of chromium at 600 nm. Completely opposite situation is observed for BGG glass triply doped with $Cr^{3+}/Er^{3+}/Ho^{3+}$, where the $^4I_{13/2}$ lifetime of Er^{3+} is reduced from 5.3 ms (0.25Cr-0.5Er) to 2.8 ms (0.25Cr-0.5Er-0.5Ho) suggesting the presence of energy transfer in direction $Er^{3+} \rightarrow Ho^{3+}$. It is also interesting to see which the energy transfer process $Yb^{3+} \rightarrow Er^{3+}$ or $Er^{3+} \rightarrow Ho^{3+}$ is more efficient for BGG glass triply doped with $Cr^{3+}/Er^{3+}/Ln^{3+}$ (Ln = Yb, Ho). For that reason, luminescence decay curves have been examined using the Inokuti-Hirayama model in order to evaluate the donor-acceptor energy transfer microparameter (C_{D-A}) and to understand excitation energy transfer mechanisms $^2F_{5/2}$ (Yb^{3+}) → $^4I_{11/2}$ (Er^{3+}) and $^4I_{13/2}$ (Er^{3+}) → $^5I_7$ (Ho^{3+}) involved in both BGG glass systems co-activated with $Cr^{3+}/Yb^{3+}/Er^{3+}$ and $Cr^{3+}/Er^{3+}/Ho^{3+}$. Previously, the Inokuti-Hirayama model has been successfully applied to explain the energy transfer processes in $Nd^{3+}/Yb^{3+}/Er^{3+}$ triply doped Ba-Al-metaphosphate glasses[56].

Considering the dipole–dipole interactions, decay curves for the $^4I_{13/2}$ (Er^{3+}) and $^2F_{5/2}$ (Yb^{3+}) states in 0.25Cr-0.5Er-0.5Ho and 0.25Cr-0.5Yb-0.5Er glass were fitted using the relation:

$$I(t) = A\,exp\left(-\left(\frac{t}{\tau}\right) - \alpha\left(\frac{t}{\tau}\right)^{3/s}\right) \quad (2)$$

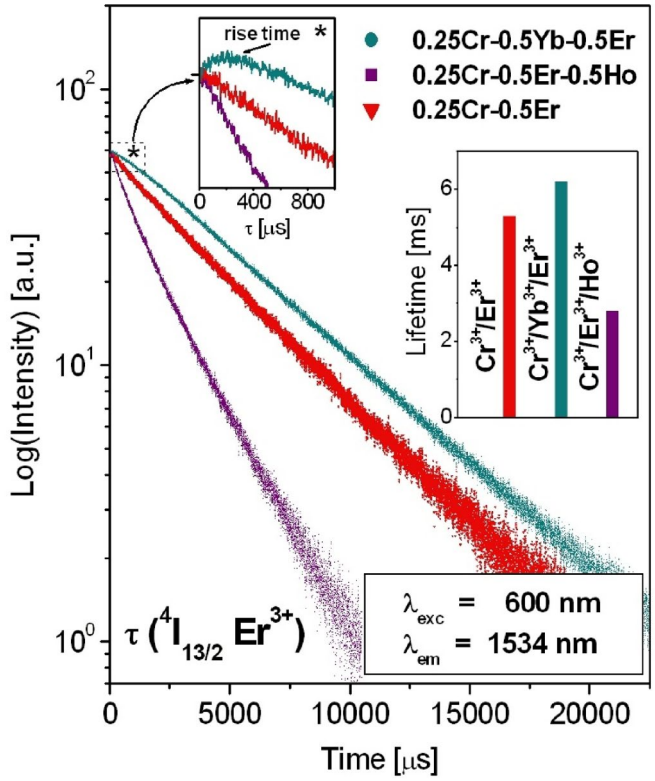


Fig. 9. Luminescence decays from $^4I_{13/2}$ excited states of Er^{3+} ions in BGG glasses doubly doped with Cr^{3+}/Er^{3+} and triply doped with $Cr^{3+}/Yb^{3+}/Er^{3+}$ and $Cr^{3+}/Yb^{3+}/Er^{3+}$. The lifetimes are also shown schematically in the inset.

Parameters	Glass code	
	0.25Cr-0.5Er-0.5Ho	0.25Cr-0.5Yb-0.5Er
Energy transfer	$^4I_{13/2}$ (Er^{3+}) → $^5I_7$ (Ho^{3+})	$^2F_{5/2}$ (Yb^{3+}) → $^4I_{11/2}$ (Er^{3+})
Ln^{3+} content [mol%]	0.5	0.5
N_A [10^{20} ions/cm^3]	2.11	2.13
τ [μs]	2800	190
α	0.35	0.4
R_0 [Å]	6.07	6.33
C_{D-A} [10^{-40} cm^6/s]	0.18	3.39

Table 2. The molar ion concentration N_A, the intrinsic lifetime of donor τ, the parameter α, the critical transfer distance R_0 and the donor-acceptor interaction parameter C_{D-A} for energy transfer processes $^4I_{13/2}$ (Er^{3+})→$^5I_7$ (Ho^{3+}) and $^2F_{5/2}$ (Yb^{3+})→$^4I_{11/2}$ (Er^{3+}) in BGG glasses triply doped with $Cr^{3+}/Er^{3+}/Ln^{3+}$ (Ln = Yb, Ho).

where: I(t) is luminescence intensity after pulse excitation, A - constant, τ – the intrinsic lifetime of donor, s = 6 for dipole-dipole interaction between the ions and α - the parameter, which is given by the expression:

$$\alpha = \frac{4}{3}\pi\left(1-\frac{3}{s}\right)N_A R_0^3 \tag{3}$$

where: Γ is the Euler function, N_A – the molar concentration of acceptor ions and R_0 denotes the critical transfer distance.

Based on relations (2) and (3) we can calculate the donor-acceptor interaction parameter C_{D-A}:

$$C_{D-A} = R_0^6 \Big/ \tau \tag{4}$$

The computational results for both energy transfer processes $^4I_{13/2}$ (Er^{3+}) → $^5I_7$ (Ho^{3+}) and $^2F_{5/2}$ (Yb^{3+}) → $^4I_{11/2}$ (Er^{3+}) in BGG glasses triply doped with $Cr^{3+}/Er^{3+}/Ln^{3+}$ ions (Ln = Yb, Ho) are summarized in Table 2.

Although the critical transfer distances R_0 for both BGG glass systems co-activated with $Cr^{3+}/Yb^{3+}/Er^{3+}$ and $Cr^{3+}/Er^{3+}/Ho^{3+}$ are similar, the donor-acceptor interaction microparameters are completely different. The value of C_{D-A} is considerably higher for 0.25Cr-0.5Yb-0.5Er glass (3.39×10^{-40} cm^6/s) than 0.25Cr-0.5Er-0.5Ho glass (0.18×10^{-40} cm^6/s). It shows that the energy transfer is more efficient for $Yb^{3+} \rightarrow Er^{3+}$ process in BGG glass co-doped with $Cr^{3+}/Yb^{3+}/Er^{3+}$ than for $Er^{3+} \rightarrow Ho^{3+}$ process in glass sample with $Cr^{3+}/Er^{3+}/Ho^{3+}$ ions. Based on literature data it is well known that the energy transfer microparameters calculated for rare earth co-doped glasses are usually situated in the range from 10^{-41} cm^6/s to 10^{-39} cm^6/s assuming dipole-dipole type interactions. Generally, the values of C_{D-A} for the studied glass systems in the presence of Cr^{3+} ions are smaller compared to the published results for glasses co-doped with Yb^{3+}/Er^{3+} and Er^{3+}/Ho^{3+} ions. For example, the energy transfer microparameter equal to 3.39×10^{-40} cm^6/s for our 0.25Cr-0.5Yb-0.5Er glass is smaller than the results ($C_{D-A} = 7.32\times10^{-40}$ cm^6/s) obtained for Yb^{3+}/Er^{3+} co-doped bismuth germanate glass[61].

At this moment it should be also noted that the energy transfer $Yb^{3+} \rightarrow Er^{3+}$ is a nearly resonant. The emission band of donor due to $^2F_{5/2} \rightarrow {}^2F_{7/2}$ transition of Yb^{3+} is well overlapped with the absorption band related to $^4I_{15/2} \rightarrow {}^4I_{11/2}$ transition of Er^{3+} ions leading to $Yb^{3+} \rightarrow Er^{3+}$ resonant energy transfer (RET) with relatively high efficiency. In some cases, the efficiency is limited by the back energy transfer $^4I_{11/2}$ (Er^{3+}) $\rightarrow {}^2F_{5/2}$ (Yb^{3+}), when it is a resonant process and has a high probability[62]. The back energy transfer process is reduced significantly with the increasing nonradiative multiphonon relaxation (MPR) rate (from the $^4I_{11/2}$ state to the lower-lying $^4I_{13/2}$ state of Er^{3+}), which depend critically on the vibrational energy of the glass host varying from nearly 1400 cm^{-1} for high-phonon oxide borate based glasses to about 500 cm^{-1} for low-phonon fluoride based glasses. Further investigations revealed that the back energy transfer for higher-phonon oxide glass host matrices has found to be negligible from estimated critical interaction distances for forward ($Yb^{3+} \rightarrow Er^{3+}$) and backward ($Er^{3+} \rightarrow Yb^{3+}$) energy transfer processes[63]. The forward energy transfer ($Yb^{3+} \rightarrow Er^{3+}$) and the back energy transfer ($Er^{3+} \rightarrow Yb^{3+}$) coefficients for Yb^{3+}/Er^{3+} co-doped BGG glass are found to be 9.2×10^{-17} cm^3/s and 1.1×10^{-17} cm^3/s, respectively[64]. Thus, the back transfer ratio for Yb^{3+}/Er^{3+} co-doped BGG glass is close to 0.12 and its value is rather low in comparison to the results 0.67 and 0.83 for pair Yb^{3+}/Er^{3+} in ZBLAN fluoride glass[65] and PbO-Bi_2O_3-Ga_2O_3 glass referred as PBG[66], for which the backward energy transfer process from Er^{3+} to Yb^{3+} ions should not be ignored. These phenomena were also confirmed for some low-phonon fluoride glass systems such as lead fluoroindogallate glasses[67] and fluoroindate glasses[68] co-doped with Yb^{3+}/Er^{3+}.

Contrary to Yb^{3+}/Er^{3+} co-doped system, spectral overlap between the emission band of donor related to $^4I_{13/2} \rightarrow {}^4I_{15/2}$ transition of Er^{3+} ions at 1534 μm (6519 cm^{-1}) and the absorption band of acceptor attributed to $^5I_8 \rightarrow {}^5I_7$ transition of Ho^{3+} ions at about 2000 nm (5000 cm^{-1}) is rather poor. Energy separation between two interacting $^4I_{13/2}$ (Er^{3+}) and $^5I_7$ (Ho^{3+}) excited states is higher than $\Delta E = 1500$ cm^{-1} suggesting the presence of non-resonant phonon-assisted energy transfer process (PAET) in Er^{3+}/Ho^{3+} co-doped glass systems.

BGG glass co-activated with $Cr^{3+}/Er^{3+}/Ho^{3+}$ ions exhibits low donor-acceptor interaction microparameter $C_{D-A} = 1.8\times10^{-41}$ cm^6/s (Table 2) related to the non-resonant energy transfer process $^4I_{13/2}$ (Er^{3+}) $\rightarrow {}^5I_7$ (Ho^{3+}) and its calculated value is less than 10^{-40} cm^6/s. Similar data were obtained for Er^{3+}/Ho^{3+} co-doped tellurite glass[69] with C_{D-A} close to 8.6×10^{-41} cm^6/s. However, donor-acceptor energy transfer parameters for Er^{3+}/Ho^{3+} co-doped glass systems are usually higher and their values C_{D-A} are above 1×10^{-40} cm^6/s. For example, the values of C_{D-A} are close to 1.01×10^{-40} cm^6/s for fluorotellurite glass[70], 2.18×10^{-40} cm^6/s for lead silicate glass[71] and 5.52×10^{-40} cm^6/s for multicomponent silicate glass[72] co-doped with Er^{3+}/Ho^{3+}.

To summarize, the calculations clearly indicated that the energy transfer coefficient C_{D-A} is higher for $Yb^{3+} \rightarrow Er^{3+}$ than $Er^{3+} \rightarrow Ho^{3+}$. Thus, near-infrared luminescence at 1534 nm is enhanced greatly for Cr^{3+}/Er^{3+} co-doped glass sample with the presence of Yb^{3+} ions. Previous studies have shown the sensitizing effect of Yb^{3+} ions on near-infrared luminescence of Er^{3+} ions at 1.5 μm in lead phosphate glass[73], alkaline-earth chloro borate glass[74] and tungsten tellurite glass[75], which were proposed for tunable laser sources and broadband optical amplifiers emitting in the infrared. Some spectroscopic parameters such as the luminescence linewidth (FWHM) and lifetime (τ) for the $^4I_{13/2} \rightarrow {}^4I_{15/2}$ transition of Er^{3+} ions in $Cr^{3+}/Yb^{3+}/Er^{3+}$ co-doped BGG glass are compared to similar glass systems. The results are given in Table 3.

It is worth noting that the measured luminescence lifetime $^4I_{13/2}$ (Er^{3+}) in $Cr^{3+}/Yb^{3+}/Er^{3+}$ co-doped BGG glass is longer compared to Er^{3+}/Yb^{3+} co-doped germanate based glasses and other oxide glass systems shown

Glass host	Activators	Spectroscopic parameters		Ref.
		FWHM [nm]	τ [ms]	
BGG	$Cr^{3+}/Yb^{3+}/Er^{3+}$	43	6.2	This work
BGG	Yb^{3+}/Er^{3+}	-	5.78	64
BGG	Yb^{3+}/Er^{3+}	37	4.01	25
GeO_2-NaO-Nb_2O_5	Yb^{3+}/Er^{3+}	44	5.24	62
Lead phosphate	Yb^{3+}/Er^{3+}	47	2.83	73
Tungsten tellurite	Yb^{3+}/Er^{3+}	59	3.96	75
Fluorotellurite	Yb^{3+}/Er^{3+}	55	10.41	15
Borosilicate	$Ce^{3+}/Yb^{3+}/Er^{3+}$	80.75	0.80	17

Table 3. Some spectroscopic parameters (FWHM, τ) for the $^4I_{13/2} \rightarrow {}^4I_{15/2}$ transition of Er^{3+} ions at 1534 nm for $Cr^{3+}/Yb^{3+}/Er^{3+}$ co-doped BGG glass compared to similar glass systems published previously.

in Table 3, but shorter than for fluorotellurite glass doubly doped with Yb^{3+}/Er^{3+}.[15] Interestingly, borosilicate glass triply doped with $Ce^{3+}/Yb^{3+}/Er^{3+}$ exhibits short-lived (0.8 ms) and broadband (above 80 nm) near-infrared luminescence near 1.55 μm.[17]

Contrary to $Cr^{3+}/Yb^{3+}/Er^{3+}$ glass system, near-infrared luminescence at 1534 nm is quenched and part of the excitation energy is transferred from $^4I_{13/2}$ state of Er^{3+} to $^5I_7$ state of Ho^{3+}. Consequently, near-infrared luminescence of holmium ions at 2000 nm in $Cr^{3+}/Er^{3+}/Ho^{3+}$ glass system should be enhanced. Figure 10 presents near-infrared luminescence spectra at 2000 nm and decay curves for BGG glasses co-doped with Cr^{3+}/Ho^{3+} and $Cr^{3+}/Er^{3+}/Ho^{3+}$. Near-infrared luminescence at 2000 nm assigned to $^5I_7 \rightarrow {}^5I_8$ transition of Ho^{3+} was increased for Cr^{3+}/Ho^{3+} co-doped glass with the presence of Er^{3+} ions confirming the energy transfer $Er^{3+} \rightarrow Ho^{3+}$.

Luminescence decay curves for BGG glasses co-doped with Cr^{3+}/Ho^{3+} and $Cr^{3+}/Er^{3+}/Ho^{3+}$ were measured under direct excitation of Cr^{3+} at 600 nm and monitoring emission wavelength 2000 nm. Decay curves for 0.25Cr-0.5Ho and 0.25Cr-0.5Er-0.5Ho co-activated glass samples become biexponential with short-lived and long-lived components. Short-lived component is due to luminescence decay of Cr^{3+} ions, whereas long-lived component of decay is changed for glass samples with the absence and presence of Er^{3+} ions. Its experimental value increases from 2820 μs (0.25Cr-0.5Ho) to 3930 μs (0.25Cr-0.5Er-0.5Ho). Further decay curve measurements under direct excitation of holmium at 450 nm and monitoring emission wavelength 2000 nm indicated that long-lived component corresponds to emission decay from the $^5I_7$ state of Ho^{3+}.

Luminescence linewidth (FWHM) and lifetime (τ) for the $^5I_7 \rightarrow {}^5I_8$ transition of Ho^{3+} ions in $Cr^{3+}/Er^{3+}/Ho^{3+}$ co-doped BGG glass are also compared to similar glass systems. The results are presented in Table 4. Although the spectral linewidths are similar (FWHM = 170÷175), the luminescence lifetime $^5I_7$ (Ho^{3+}) in $Cr^{3+}/Er^{3+}/Ho^{3+}$ co-doped BGG glass is longer compared to Cr^{3+}/Ho^{3+} co-doped BGG glass modified with BaF_2,[76] and other oxide glass systems shown in Table 4, but shorter than for BGG glass doubly doped with Er^{3+}/Ho^{3+} ions.[26] Further analysis indicates that the introduction of Tm^{3+} to glass systems containing pairs Cr^{3+}/Ho^{3+} or Er^{3+}/Ho^{3+} influenced greatly on their ultrabroadband near-IR emission properties (FWHM above 300 nm). It was confirmed for $Cr^{3+}/Tm^{3+}/Ho^{3+}$ co-doped BGG glass[49] as well as tellurite[77] and germanate (BGG)[33] glass systems triply doped with $Er^{3+}/Tm^{3+}/Ho^{3+}$ ions. On the other hand, the enhanced long-lived (τ > 10 ms) near-infrared luminescence of Ho^{3+} ions near 2 μm was observed for Er^{3+}/Ho^{3+} co-doped fluorotellurite glass[70] and fluoride glass systems (ZBYA) containing Er^{3+}/Ho^{3+} and $Ce^{3+}/Er^{3+}/Ho^{3+}$ ions.[78]

Finally, the excitation spectra for BGG glasses with Cr^{3+} and Ln^{3+} (Ln = Er and/or Yb, Ho) were registered under selective monitoring emission wavelengths in order to confirm the presence of energy transfer processes. The excitation spectra are presented in Fig. 11.

The excitation spectra for BGG glasses triply doped with $Cr^{3+}/Yb^{3+}/Er^{3+}$ were measured selectively under monitoring emission wavelengths at 1534 nm (Er^{3+}) and 1020 nm (Yb^{3+}), whereas the spectra for glass samples co-activated with $Cr^{3+}/Er^{3+}/Ho^{3+}$ ions were monitored at λ_{em} = 1534 nm (Er^{3+}) and λ_{em} = 2000 nm (Ho^{3+}). In

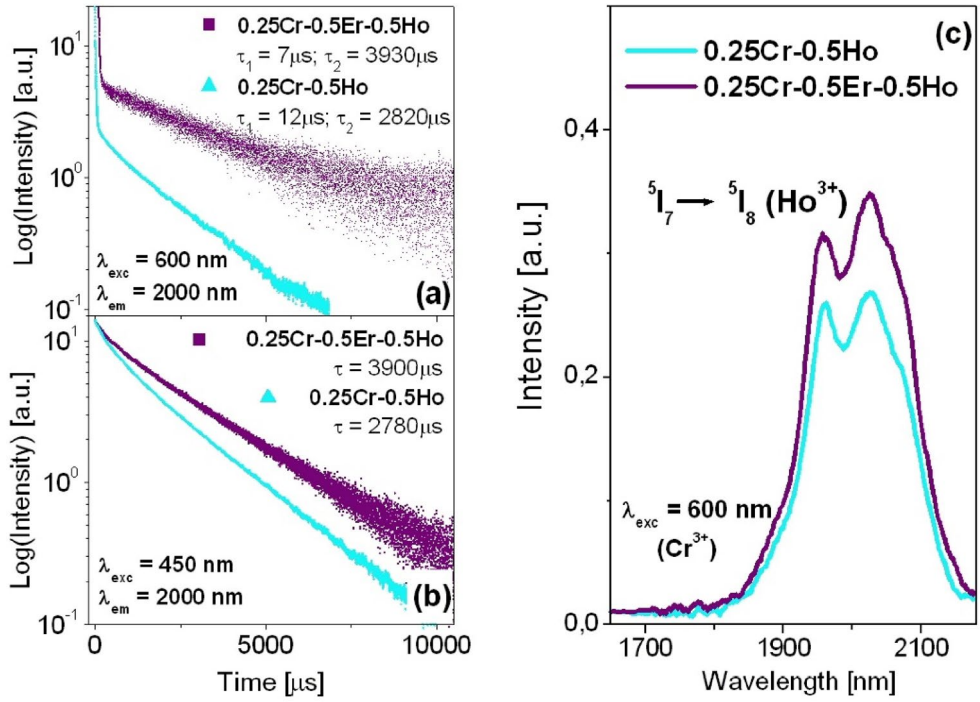


Fig. 10. Luminescence decays for BGG glasses co-doped with Cr^{3+}/Ho^{3+} and $Cr^{3+}/Er^{3+}/Ho^{3+}$ measured under direct excitation of (**a**) Cr^{3+} at 600 nm and (**b**) Ho^{3+} at 450 nm and (**c**) near-infrared luminescence spectra of Ho^{3+}.

Glass host	Activators	Spectroscopic parameters		Ref.
		FWHM [nm]	τ [ms]	
BGG	$Cr^{3+}/Er^{3+}/Ho^{3+}$	170	3.93	this work
BGG-BaF_2	Cr^{3+}/Ho^{3+}	175	2.57	76
BGG	Er^{3+}/Ho^{3+}	-	5.67	26
Lead silicate	Er^{3+}/Ho^{3+}	175	0.88	58
Germano-silicate	Er^{3+}/Ho^{3+}	-	1.92	60
Tellurite	$Er^{3+}/Tm^{3+}/Ho^{3+}$	374	-	77
BGG	$Er^{3+}/Tm^{3+}/Ho^{3+}$	340	5.27	33
BGG	$Cr^{3+}/Tm^{3+}/Ho^{3+}$	339	-	49
Fluorotellurite	Er^{3+}/Ho^{3+}	-	11.7	70
Fluoride (ZBYA)	Er^{3+}/Ho^{3+}	-	18.2	78
Fluoride (ZBYA)	$Ce^{3+}/Er^{3+}/Ho^{3+}$	-	21.4	78

Table 4. Some spectroscopic parameters (FWHM, τ) for the $^5I_7 \rightarrow {}^5I_8$ transition of Ho^{3+} ions at 2000 nm for $Cr^{3+}/Er^{3+}/Ho^{3+}$ co-doped BGG glass compared to similar glass systems published previously.

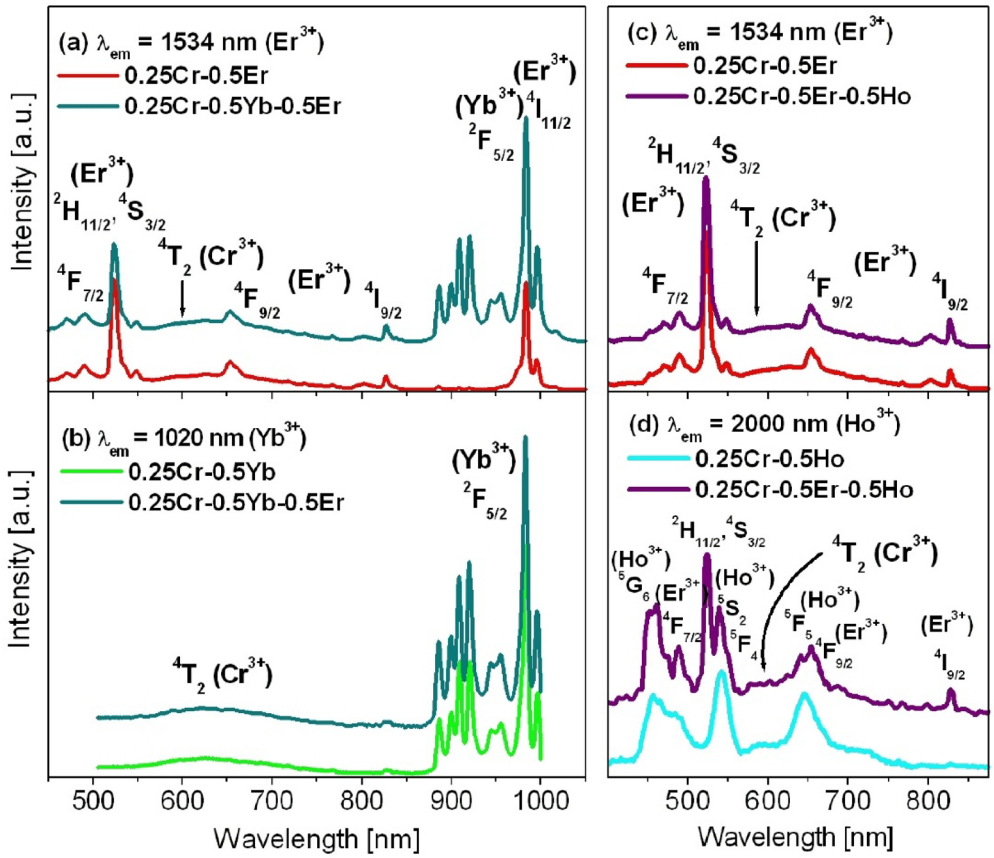


Fig. 11. Excitation spectra for BGG glasses containing Cr^{3+} and Ln^{3+} (Ln = Er and/or Yb, Ho) ions measured under selective monitoring emission wavelengths.

order to identify excitation bands, the results for samples co-doped with Cr^{3+}/Ln^{3+} (Ln = Er, Yb, Ho) are also given. In all cases, the presence of characteristic bands of Ln^{3+} ions lying on the low-intensity broad excitation band of Cr^{3+} centered at about 600 nm confirms the energy transfer process in direction from chromium ions playing the role as a donor to rare earth ions (acceptors).

In particular, the excitation spectra for 0.25Cr-0.5Er and 0.25Cr-0.5Yb-0.5Er glass samples measured under monitoring emission wavelength at 1534 nm (Er^{3+}) consist of bands originating to transitions from the $^4I_{15/2}$ ground state to the higher-lying states of Er^{3+} as well as $^4A_2 \rightarrow {}^4T_2$ transition of Cr^{3+} ions. Also, the additional band related to $^2F_{7/2} \rightarrow {}^2F_{5/2}$ transition of Yb^{3+} ions is quite well observed for 0.25Cr-0.5Yb-0.5Er glass contrary

to 0.25Cr-0.5Er glass sample. It indicates that the following energy transfer processes $Cr^{3+} \rightarrow Er^{3+}$ and $Cr^{3+} \rightarrow Yb^{3+} \rightarrow Er^{3+}$ are present in BGG glasses. The excitation spectra for 0.25Cr-0.5Yb and 0.25Cr-0.5Yb-0.5Er glass samples registered under monitoring emission wavelength at 1020 nm (Yb^{3+}) consist of characteristic bands of Cr^{3+} and Yb^{3+} ions. It suggests the presence of energy transfer process from Cr^{3+} (donor) to Yb^{3+} ions (acceptor) and the absence of back energy transfer $Er^{3+} \rightarrow Yb^{3+}$. Compared to 0.25Cr-0.5Er co-doped sample, the excitation spectrum for 0.25Cr-0.5Er-0.5Ho glass measured under monitoring emission wavelength at 1534 nm (Er^{3+}) is nearly the same indicating that the energy transfer process in direction $Cr^{3+} \rightarrow Er^{3+}$ occurs. Further analysis for 0.25Cr-0.5Ho and 0.25Cr-0.5Er-0.5Ho glass samples under monitoring emission wavelength at 2000 nm (Ho^{3+}) gives interesting results. The excitation spectrum for 0.25Cr-0.5Ho sample consists of characteristic bands of Cr^{3+} and Ho^{3+} confirming the energy transfer $Cr^{3+} \rightarrow Ho^{3+}$. For 0.25Cr-0.5Er-0.5Ho co-activated glass, both characteristic bands of Er^{3+} and Ho^{3+} are lying on the broad band of Cr^{3+} suggesting the presence of energy transfer processes $Cr^{3+} \rightarrow Ho^{3+}$ and $Cr^{3+} \rightarrow Er^{3+} \rightarrow Ho^{3+}$. The results quite well demonstrate the presence of energy transfer processes from Yb^{3+} (donor) to Er^{3+} (acceptor) and from Er^{3+} (donor) to Ho^{3+} (acceptor) in the excitation spectra measured for $Cr^{3+}/Er^{3+}/Ln^{3+}$ (Ln = Yb, Ho) triply doped BGG glasses under monitoring emission wavelengths at 1534 nm (Er^{3+}) and 2000 nm (Ho^{3+}), respectively. It is also well collaborates with the results obtained from the luminescence decay curve measurements.

Conclusions

Barium gallo-germanate glasses (BGG) co-activated with Cr^{3+}/Er^{3+} and $Cr^{3+}/Er^{3+}/Ln^{3+}$ ions (Ln = Yb, Ho) have been studied for near-infrared luminescence applications. Near-infrared luminescence properties have been examined for BGG glasses excited directly at 600 nm (Cr^{3+}). Near-infrared luminescence corresponding to $^4I_{13/2} \rightarrow {}^4I_{15/2}$ transition of Er^{3+} ions is enhanced greatly for $Cr^{3+}/Yb^{3+}/Er^{3+}$ glass, whereas luminescence quenching of Er^{3+} ions at 1534 nm and enhancement of Ho^{3+} at 2000 nm is quite well observed for $Cr^{3+}/Er^{3+}/Ho^{3+}$ glass, respectively. The radiative/non-radiative mechanisms and the energy transfer channels in $Cr^{3+}/Yb^{3+}/Er^{3+}$ and $Cr^{3+}/Er^{3+}/Ho^{3+}$ triply doped BGG glasses are proposed. Based on emission spectra and decays, the energy transfer processes $Cr^{3+} \rightarrow Yb^{3+} \rightarrow Er^{3+}$ and $Cr^{3+} \rightarrow Er^{3+} \rightarrow Ho^{3+}$ were identified. The energy transfer efficiencies for glasses triply doped with $Cr^{3+}/Yb^{3+}/Er^{3+}$ and $Cr^{3+}/Er^{3+}/Ho^{3+}$ are close to nearly 55% ± 1%. The energy transfer coefficients for both processes $Yb^{3+} \rightarrow Er^{3+}$ and $Er^{3+} \rightarrow Ho^{3+}$ present in BGG glasses with $Cr^{3+}/Er^{3+}/Ln^{3+}$ (Ln = Yb, Ho) were determined. The energy transfer microparameter is larger for $Yb^{3+} \rightarrow Er^{3+}$ than $Er^{3+} \rightarrow Ho^{3+}$ process. The presence of energy transfer processes was also verified by the excitation spectra measurements. The results demonstrate that BGG glasses co-activated with $Cr^{3+}/Yb^{3+}/Er^{3+}$ and $Cr^{3+}/Er^{3+}/Ho^{3+}$ are attractive for near-infrared luminescence under direct excitation of Cr^{3+} ions at 600 nm.

Methods

Synthesis

Barium gallo-germanate glasses (BGG) triply doped with $Cr^{3+}/Yb^{3+}/Er^{3+}$ and $Cr^{3+}/Er^{3+}/Ho^{3+}$ ions were prepared in a glove-box under an atmosphere dry argon to minimize the OH^- groups. In order to compare luminescence properties, BGG glasses singly doped with Cr^{3+} and doubly doped with Cr^{3+}/Ln^{3+} (Ln = Er, Yb, Ho) were also synthesized. Chemical compositions of glass samples (in mol %) are as follows: $60GeO_2–30BaO-8.75Ga_2O_3–0.25Cr_2O_3–0.5Er_2O_3–0.5Ln_2O_3$ and $60GeO_2–30BaO-9.25Ga_2O_3–0.25Cr_2O_3–0.5Ln_2O_3$ (where Ln denotes Yb or Ho) as well as $60GeO_2–30BaO-9.75Ga_2O_3–0.25Cr_2O_3$ and $60GeO_2–30BaO-(9.75-x)Ga_2O_3–0.25Cr_2O_3-xEr_2O_3$ (where x = 0.1, 0.5 and 1.0). Also, Eu^{3+}-doped BGG glass with the following composition $60GeO_2–30BaO-9.5Ga_2O_3–0.5Eu_2O_3$ was prepared in order to determine the phonon energy of the glass-host. High-purity components (99.99% Aldrich Chemical Co.) used for glass preparation were mixed homogenously together. Next, the mixture was charged into a covered platinum crucible and melted in a high-temperature electrical furnace (FCF 4/170 M produced by Czylok, Jastrzębie Zdrój, Poland) at T = 1200 °C for 0.45 h. Finally, the samples were annealed below the glass transition temperature to minimize internal mechanical stress during the quenching process. Each glass sample was polished for luminescence measurements.

Measurement and characterization

In order to characterize glass samples, DSC curves, the Raman spectra and the X-ray diffraction patterns were measured using SETARAM Labsys analyzer, Thermo Scientific™ DXR™2xi Raman imaging microscope and X'Pert-Pro diffractometer with CuKα radiation (PANalytical, Eindhoven, The Netherlands). The DSC curves were acquired with standard heating rate of 10 °C/min, whereas characteristic temperatures and thermal stability parameter were determined within an accuracy of ± 0.5 °C. Spectrophotometer Cary 5000 UV–VIS–NIR supplied by Agilent Technology (USA) was used to measure the absorption spectra. The excitation and emission spectra were registered using PTI QuantaMaster QM40 spectrofluorometer (Photon Technology International, Birmingham, NJ, USA), which includes a xenon lamp (75 W), double 200 mm monochromator, Hamamatsu H10330B-75 and InGaAs detectors. Resolution for the spectra measurements was ± 0.1 nm. For emission decay curve measurements, pulsed tunable optical parametric oscillator (OPO) pumped by the third harmonic of a Nd: YAG laser (Opotek Opolette 355 LD, OPOTEK, Carlsbad CA, USA) was used. Decay curves with an accuracy of ± 0.1 μs were recorded using the PTI ASOC-10 USB-2500 oscilloscope (Horiba Instruments).

Data availability

All data regarding the work presented here is available upon reasonable request to the corresponding author.

Received: 27 April 2026; Accepted: 4 August 2026
Published online: 08 August 2026

References

1. Blanc, W. et al. The past, present and future of photonic glasses: A review in homage to the United Nations International Year of glass 2022. *Prog Mater. Sci.* **134**, 101084. https://doi.org/10.1016/j.pmatsci.2023.101084 (2023).
2. Jha, A. et al. Rare-earth ion doped TeO_2 and GeO_2 glasses as laser materials. *Prog Mater. Sci.* **57**, 1426–1491. https://doi.org/10.1016/j.pmatsci.2012.04.003 (2012).
3. Frigenti, G. et al. Rare earth-doped glass whispering gallery mode micro-lasers. *Eur. Phys. J. Plus.* **138**, 679. https://doi.org/10.1140/epjp/s13360-023-04275-9 (2023).
4. Ekim, U., Özkutay, D., Ersundu, M. C. & Ersundu, A. E. Full-color dynamic volumetric displays with tunable upconversion emission from RE^{3+}-doped glasses (RE = Ho, Tm, Nd, Yb) under NIR laser excitation. *Light: Sci. Appl.* **14**, 15. https://doi.org/10.1038/s41377-024-01672-2 (2025).
5. Zhu, Y. & Deng, R. Colour triad in rare-earth doped glass: a step toward volumetric displays. *Light: Sci. Appl.* **14**, 84. https://doi.org/10.1038/s41377-025-01763-8 (2025).
6. Zhang, Q., Chen, G., Zhang, G., Qiu, J. & Chen, D. Infrared luminescence of Tm^{3+}/Yb^{3+} codoped lanthanum aluminum germanate glasses. *J. Appl. Phys.* **107**, 023102. https://doi.org/10.1063/1.3289589 (2010).
7. Zhou, B., Tao, L., Tsang, Y. H., Jin, W. & Pun E.Y.B. Superbroadband near-infrared emission and energy transfer in Pr^{3+}-Er^{3+} codoped fluorotellurite glasses. *Opt. Express.* **20**, 12205–12211. https://doi.org/10.1364/OE.20.012205 (2012).
8. Sousa, J. F., Alves, R. T., Rego-Filho, F. G. & Gouveia-Neto, A. S. Erbium-to-dysprosium energy-transfer mechanism and visible luminescence in lead-cadmium-fluorogermanate glass excited at 405 nm. *Chem. Phys. Lett.* **723**, 28–32. https://doi.org/10.1016/j.cplett.2019.03.017 (2019).
9. Pisarski, W. A. et al. Fluoroindate glasses co–doped with Pr^{3+}/Er^{3+} for near–infrared luminescence applications. *Sci. Rep.* **10**, 21105. https://doi.org/10.1038/s41598-020-77943-w (2020).
10. Gouveia-Neto, A. S. et al. White light generation by frequency upconversion in $Tm^{3+}/Ho^{3+}/Yb^{3+}$ - codoped fluorolead germanate glass. *Appl. Phys. Lett.* **91**, 091114. https://doi.org/10.1063/1.2775043 (2007).
11. Manzani, D. et al. Yb^{3+}, Tm^{3+} and Ho^{3+} triply-doped tellurite core cladding optical fiber for white light generation. *Opt. Mater. Exp.* **1**, 1515–1526. https://doi.org/10.1364/OME.1.001515 (2011).
12. Capelo, R. G. et al. Blue upconversion emission of $Nd^{3+}/Tm^{3+}/Yb^{3+}$ triply doped aluminophosphate optical fibers. *ACS Appl. Opt. Mater.* **2**, 2501–2508. https://doi.org/10.1021/acsaom.4c00348 (2024).
13. Ribeiro, C. T. B., Zanatta, A. R., Nunes, L. A. O., Messaddeq, Y. & Aegerter, M. A. Optical spectroscopy of Er^{3+} and Yb^{3+} co-doped fluoroindate glasses. *J. Appl. Phys.* **83**, 2256–2260. https://doi.org/10.1063/1.366965 (1998).
14. Manzani, D., Ferrari, J. L., Polachini, F. C., Messaddeq, Y. & Ribeiro, S. J. L. 1.5 μm and visible up-conversion emissions in Er^{3+}/Yb^{3+} co-doped tellurite glasses and optical fibers for photonic applications. *J. Mater. Chem.* **22**, 16540–16545. https://doi.org/10.1039/C2JM33057A (2012).
15. Huang, F. et al. Origin of near to middle infrared luminescence and energy transfer process of Er^{3+}/Yb^{3+} co-doped fluorotellurite glasses under different excitations. *Sci. Rep.* **5**, 8233. https://doi.org/10.1038/srep08233 (2015).
16. Manzani, D., da Silveira Petruci, J. F., Nigoghossian, K., Cardoso, A. A. & Ribeiro, S. J. L. A portable luminescent thermometer based on green upconversion emission of Er^{3+}/Yb^{3+} co-doped tellurite glass. *Sci. Rep.* **7**, 41596. https://doi.org/10.1038/srep41596 (2017).
17. Chu, Y. et al. Ce3+/Yb3+/Er3+ triply doped bismuth borosilicate glass: a potential fiber material for broadband near-infrared fiber amplifiers. *Sci. Rep.* https://doi.org/10.1038/srep33865 (2016).
18. Ma, Y., Huang, F., Hu, L. & Zhang, J. Efficient 2.05 μm emission of $Ho^{3+}/Yb^{3+}/Er^{3+}$ triply doped fluorotellurite glasses. *Spectrochim Acta A.* **122**, 711–714. https://doi.org/10.1016/j.saa.2013.11.103 (2014).
19. Bayya, S. S., Chin, G. D., Sanghera, J. S. & Aggarwal, I. D. Germanate glass as a window for high energy laser systems. *Opt. Express.* **19**, 6514–6523. https://doi.org/10.1364/OE.14.011687 (2011).
20. Wen, X. et al. Tm^{3+} doped barium gallo-germanate glass single mode fibers for 2.0 μm laser. *Opt. Express.* **23**, 7722–7731. https://doi.org/10.1364/OE.23.007722 (2015).
21. Pisarska, J. et al. Influence of BaF_2 and activator concentration on broadband near-infrared luminescence of Pr^{3+} ions in gallo-germanate glasses. *Opt. Express.* **24**, 2427–2435. https://doi.org/10.1364/OE.24.002427 (2016).
22. Tang, G. et al. Yang, Z. Tm^{3+}-doped barium gallo-germanate glass single-mode fiber with high gain per unit length for ultracompact 1.95μm laser. *Appl. Phys. Exp.* **11**, 032701. https://doi.org/10.7567/APEX.11.032701 (2018).
23. Tang, G. et al. Structure and luminescence properties of Tm^{3+} doped barium gallo-germanate glass tailored by Lu_2O_3. *J. Lumin.* **257**, 119771. https://doi.org/10.1016/j.jlumin.2023.119771 (2023).
24. Calzavara, F. et al. Dehydration processing of Er3+-doped barium gallo-germanate glasses with ultra-low hydroxyl absorption for near and mid-infrared applications. *Opt. Mater.* https://doi.org/10.1016/j.optmat.2025.117096 (2025).
25. Xiao, K. & Yang, Z. Thermal stability and optical transitions of Er^{3+}/Yb^{3+}-codoped barium gallogermanate glass. *Opt. Mater.* **29**, 1475–1480. https://doi.org/10.1016/j.optmat.2006.07.009 (2007).
26. Tang, G. et al. Efficient 2.0 μm emission in Er^{3+}/Ho^{3+} co-doped barium gallo-germanate glasses under different excitations for mid-infrared laser. *J. Alloys Compd.* **664**, 19–24. https://doi.org/10.1016/j.jallcom.2015.12.205 (2016).
27. Kochanowicz, M. et al. D. 2 μm emission in gallo-germanate glasses and glass fibers co-doped with Yb^{3+}/Ho^{3+} and $Yb^{3+}/Tm^{3+}/Ho^{3+}$. *J. Lumin.* **211**, 341–346. https://doi.org/10.1016/j.jlumin.2019.03.060 (2019).
28. Leonov, S., Guerineau, T., Bernier, M., Messaddeq, Y. & Vallee, R. Demonstration of a 0.8 W continuous wave bulk laser around 2 μm in a Tm^{3+}: Ga-Rich BGG glass. *Opt. Mater. Exp.* **14**, 1690–1698. https://doi.org/10.1364/OME.524064 (2024).
29. Dupont, A. et al. Lasing in a femtosecond-laser-written single-scan waveguide fabricated in Tm-doped BGG glass. *Opt. Lett.* **50**, 666–669. https://doi.org/10.1364/OL.547643 (2025).
30. Guerineau, T. et al. Extended germano-gallate fiber drawing domain: from germanates to gallates optical fibers. *Opt. Mater. Exp.* **9**, 2437–2445. https://doi.org/10.1364/OME.9.002437 (2019).
31. Guerineau, T., Dupont, A., Lapointe, J., Vallee, R. & Messaddeq, Y. Investigation of Ga_2O_3-BaO-GeO_2 glasses for ultrafast laser inscription. *Opt. Mater. Exp.* **13**, 2036–2052. https://doi.org/10.1364/OME.491952 (2023).
32. Guerineau, T. et al. Toward low-loss mid-infrared Ga_2O_3–BaO–GeO_2 optical fibers. *Sci. Rep.* **13**, 3697. https://doi.org/10.1038/s41598-023-30522-1 (2023).
33. Qian, G. et al. Broadband 2 μm amplified spontaneous emission of $Er^{3+}/Tm^{3+}/Ho^{3+}$ triply-doped germanate glass fiber. *J. Lumin.* **289**, 121672. https://doi.org/10.1016/j.jlumin.2025.121672 (2026).
34. Kochanowicz, M. et al. Ultra-broadband emission in $Er^{3+}/Tm^{3+}/Ho^{3+}$ triply-doped germanate glass and double-clad optical fiber. *Opt. Mater. Exp.* **12**, 2332–2342. https://doi.org/10.1364/OME.462653 (2022).
35. Markiewicz, J. et al. Broadband 1.5–2.1 μm emission in gallo-germanate dual-core optical fiber co-doped with Er^{3+} and $Yb^{3+}/Tm^{3+}/Ho^{3+}$. *Opt. Exp.* **31**, 28850–28858. https://doi.org/10.1364/OE.496574 (2023).
36. Markiewicz, J. et al. Ultrabroadband near-infrared emission profiling in multicore optical fibers doped with Er^{3+} and $Yb^{3+}/Tm^{3+}/Ho^{3+}$ ions. *Sci. Rep.* **15**, 4161. https://doi.org/10.1038/s41598-025-88411-8 (2025).
37. Pisarski, W. A., Janek, J., Pisarska, J., Lisiecki, R. & Ryba-Romanowski, W. Influence of temperature on up-conversion luminescence in Er^{3+}/Yb^{3+} doubly doped lead-free fluorogermanate glasses for optical sensing. *Sens. Actuat B.* **253**, 85–91. https://doi.org/10.1016/j.snb.2017.06.074 (2017).
38. Markiewicz, J. et al. Broadband near-infrared emission in barium gallo-germanate glasses and multicore fibers co-doped with bismuth, chromium and rare-earth ions. *Ceram. Int.* **51**, 16621–16628. https://doi.org/10.1016/j.ceramint.2025.02.248 (2025).

39. Ye, S. et al. Broadband Cr^{3+}-sensitized upconversion luminescence in $La_3Ga_5GeO_{14}$:Cr^{3+},Yb^{3+},Er^{3+}. *Opt. Mater. Exp.* **4**, 638–648. https://doi.org/10.1364/OME.4.000638 (2014).
40. Zhang, A. et al. Simultaneous luminescence in I, II and III biological windows realized by using the energy transfer of $Yb^{3+} \rightarrow Er^{3+}$/$Ho^{3+} \rightarrow Cr^{3+}$. *Chem. Eng. J.* **365**, 400–404. https://doi.org/10.1016/j.cej.2019.02.061 (2019).
41. Gong, C. et al. Simultaneously strong NIR-II and NIR-III luminescence induced by Cr^{3+}-Yb^{3+}-Er^{3+} energy transfer in $KScP_2O_7$ for NIR thermometry, NIR pc-LED and night-vision applications. *Ceram. Int.* **50**, 35465–35473. https://doi.org/10.1016/j.ceramint.2024.06.358 (2024).
42. Guo, Y., Fu, Y. & Zhao, L. Effect of Cr^{3+} occupying an extremely weak crystal field on down-conversion of β-PbF_2:Er^{3+}/Yb^{3+}/Cr^{3+} glass–ceramic composites. *New. J. Chem.* **49**, 6621–6628. https://doi.org/10.1039/D4NJ04597A (2025).
43. Chen, D., Liu, S., Xu, W. & Li, X. Yb^{3+}/Ln^{3+}/Cr^{3+} (Ln = Er, Ho) doped transparent glass ceramics: crystallization, Ln^{3+} sensitized Cr^{3+} upconversion emission and multi-modal temperature sensing. *J. Mater. Chem. C.* **5**, 11769–11780. https://doi.org/10.1039/C7TC04410K (2017).
44. Fang, Z. et al. Optical thermometry properties of silicate glass-ceramics with dual-phase for spatial isolation of Er^{3+} and Cr^{3+}. *J. Lumin.* **219**, 116861. https://doi.org/10.1016/j.jlumin.2019.116861 (2020).
45. Ledig, M., Heumann, E., Ehrt, D. & Seeber, W. Spectroscopic and laser properties of Cr^{3+}:Yb^{3+}:Er^{3+}: fluoride phosphate glass. *Opt. Quant. Electron.* **22**, S107–S122. https://doi.org/10.1007/BF02089004 (1990).
46. Dan, H. K., Ty, N. M., Zhou, D., Qiu, J. & Phan, A. L. Influence of Cr^{3+} on yellowish-green UC emission and energy transfer of Er^{3+}/Cr^{3+}/Yb^{3+} tridoped zinc silicate glasses. *J. Am. Ceram. Soc.* **103**, 6356–6368. https://doi.org/10.1111/jace.17359 (2020).
47. Kowalska, K., Kuwik, M., Polak, J., Pisarska, J. & Pisarski, W. A. EPR and optical spectroscopy of Cr^{3+} ions in barium gallo-germanate glasses containing B_2O_3/TiO_2. *J. Lumin.* **245**, 118775. https://doi.org/10.1016/j.jlumin.2022.118775 (2022).
48. Pisarska, J. et al. Influence of transition metal ion concentration on near-infrared emission of Ho^{3+} in barium gallo-germanate glasses. *J. Alloys Compd.* **793**, 107–114. https://doi.org/10.1016/j.jallcom.2019.04.154 (2019).
49. Pisarski, W. A., Kuwik, M. & Pisarska, J. Cr^{3+}/Tm^{3+}/Ho^{3+} triply doped barium gallo-germanate glasses for near-infrared luminescence applications. *Ceram. Int.* **51**, 46184–46189. https://doi.org/10.1016/j.ceramint.2025.07.270 (2025).
50. Linganna, K. et al. Optical properties of Er^{3+}-doped K-Ca-Al fluorophosphate glasses for optical amplification at 1.53 μm. *Opt. Mater. Exp.* **5**, 1689–1703. https://doi.org/10.1364/OME.5.001689 (2015).
51. Linganna, K. et al. V. 1.53 μm luminescence properties of Er^{3+}-doped K–Sr–Al phosphate glasses. *Ceram. Int.* **41**, 5765–5771. https://doi.org/10.1016/j.ceramint.2014.12.162 (2015).
52. Nayab Rasool, S., Jamalaiah, B. C., Suresh, K., Rama Moorthy, L. & Jayasankar, C. K. Spectroscopic properties of Er^{3+}-doped phosphate based glasses for broadband 1.54 μm emission. *J. Mol. Struct.* **1130**, 837–843. https://doi.org/10.1016/j.molstruc.2016.10.090 (2017).
53. Damodaraiah, S., Reddy Prasad, V. & Ratnakaram, Y. C. Investigation of Green and 1.53 μm emission characteristics of Er^{3+} doped bismuth phosphate glasses for laser applications. *J. Alloys Compd.* **741**, 269–280. https://doi.org/10.1016/j.jallcom.2018.01.158 (2018).
54. Jose, A. et al. Spectroscopic investigations on 1.53 μm NIR emission of Er^{3+} doped multicomponent borosilicate glasses for telecommunication and lasing applications. *Mater. Chem. Phys.* **261**, 124223. https://doi.org/10.1016/j.matchemphys.2021.124223 (2021).
55. Kostka, P., Yatskiv, R., Grym, J. & Zavadil, J. Enhancing near-infrared emission in Nd^{3+}/Er^{3+} tellurite glasses through Cr^{3+} co-doping. *Ceram. Int.* **52**, 11953–11958. https://doi.org/10.1016/j.ceramint.2026.01.352 (2026).
56. Sontakke, A. D., Biswas, K., Mandal, A. K. & Annapurna, K. Time resolved fluorescence and energy transfer analysis of Nd^{3+}–Yb^{3+}–Er^{3+} triply-doped Ba–Al-metaphosphate glasses for an eye safe emission (1.54 μm). *J. Fluoresc.* **20**, 425–434. https://doi.org/10.1007/s10895-009-0562-z (2010).
57. Zhang, F. F. et al. Efficient 2.0 μm fluorescence in Ho^{3+}-doped fluorogermanate glass sensitized by Cr^{3+}. *Opt. Mater. Exp.* **4**, 1404–1410. https://doi.org/10.1364/OME.4.001404 (2014).
58. Qian, G. et al. Efficient 2 μm emission in Er^{3+}/Ho^{3+} co-doped lead silicate glasses under different excitations. *Opt. Mater.* **82**, 147–153. https://doi.org/10.1016/j.optmat.2018.05.061 (2018).
59. Wang, N. et al. An efficient 2.0 μm emission of Er^{3+}/Ho^{3+} co-doped lead silicate glass. *Infrared Phys. Technol.* **83**, 1–6. https://doi.org/10.1016/j.infrared.2017.03.015 (2017).
60. Wei, T. et al. Quantitative analysis of energy transfer and origin of quenching in Er^{3+}/Ho^{3+} codoped germanosilicate glasses. *J. Phys. Chem. A.* **119**, 6823–6830. https://doi.org/10.1021/acs.jpca.5b04537 (2015).
61. Zhao, G., Wang, S., Fan, H. & Hu, L. Mid-infrared spectroscopic properties and energy transfer of Er^{3+}/Yb^{3+} co-doped bismuth germanate glass. *Spectrochim Acta A.* **101**, 49–53. https://doi.org/10.1016/j.saa.2012.09.052 (2013).
62. Ajroud, M. et al. Energy transfer processes in (Er^{3+}–Yb^{3+})-codoped germanate glasses for mid-infrared and up-conversion applications. *Mater. Sci. Eng. C.* **26**, 523–529. https://doi.org/10.1016/j.msec.2005.10.015 (2006).
63. Sontakke, A. D. & Annapurna, K. Energy transfer based efficient infrared emission at 1.57 μm from Yb^{3+}–Er^{3+} codoped Zinc-borobismuthate glasses. *Opt. Mater.* **35**, 472–478. https://doi.org/10.1016/j.optmat.2012.09.044 (2013).
64. Jiang, X. P., Yang, Z. M., Liu, T. & Xu, S. H. Energy transfer between Yb^{3+} and Er^{3+} in barium gallogermanate glass. *J. Appl. Phys.* **105**, 103113. https://doi.org/10.1063/1.3130407 (2009).
65. da Vila, L. D., Gomes, L., Tarelho, L. V. G., Ribeiro, S. J. L., Messaddeq, Y. & and Mechanism of the Yb–Er energy transfer in fluorozirconate glass. *J. Appl. Phys.* **93**, 3837–3880. https://doi.org/10.1063/1.1555679 (2003).
66. Kassab, L. R. P., Fukumoto, M. E. & Gomes, L. Energy transfer in PbO–Bi_2O_3–Ga_2O_3 glasses codoped with Yb^{3+} and Er^{3+}. *J. Opt. Soc. Amer B.* **22**, 1255–1259. https://doi.org/10.1364/JOSAB.22.001255 (2005).
67. de Sousa, D. F. et al. Er^{3+}:Yb^{3+} codoped lead fluoroindogallate glasses for mid infrared and upconversion applications. *J. Appl. Phys.* **85**, 2502–2507. https://doi.org/10.1063/1.369612 (1999).
68. Ragin, T. et al. Effect of Yb^{3+}/Er^{3+} co-doping on the emission properties of fluoroindate glass and glass optical fiber. *Ceram. Int.* **49**, 41272–41280. https://doi.org/10.1016/j.ceramint.2023.05.278 (2023).
69. Li, X. & Zhang, W. The microscopic interaction parameters for Er^{3+}/Ho^{3+} energy transfer in tellurite glasses. *Phys. B.* **403**, 2714–2728. https://doi.org/10.1016/j.physb.2008.01.041 (2008).
70. Huang, F., Liu, X., Hu, L., Chen, D. & and Optical properties and energy transfer processes of Ho^{3+}/Er^{3+}- codoped fluorotellurite glass under 1550 nm excitation for 2.0 μm applications. *J. Appl. Phys.* **116**, 033106. https://doi.org/10.1063/1.4890719 (2014).
71. Liu, X. et al. Investigation on Er^{3+}/Ho^{3+} co-doped silicate glass for ~2 μm fiber lasers. *J. Lumin.* **162**, 197–202. https://doi.org/10.1016/j.jlumin.2015.02.037 (2015).
72. Cao, R. et al. J. 2 μm emission properties and nonresonant energy transfer of Er^{3+} and Ho^{3+} codoped silicate glasses. *Sci. Rep.* **6**, 37873. https://doi.org/10.1038/srep37873 (2016).
73. Basavapoornima, C., Maheswari, T., Rani Depuru, S. & Jayasankar, C. K. Sensitizing effect of Yb^{3+} ions on photoluminescence properties of Er^{3+} ions in lead phosphate glasses: Optical fiber amplifiers. *Opt. Mater.* **86**, 256–269. https://doi.org/10.1016/j.optmat.2018.09.027 (2018).
74. Talewar, R. A., Mahamuda, S., Swapna, K., Venkateswarlu, M. & Rao, A. S. Sensitization of Er^{3+} NIR emission using Yb^{3+} ions in alkaline-earth chloro borate glasses for fiber laser and optical fiber amplifier applications. *Mater. Res. Bull.* **136**, 111144. https://doi.org/10.1016/j.materresbull.2020.111144 (2021).
75. Yuan, J. et al. Enhanced 1.5 μm emission from Yb^{3+}/Er^{3+} codoped tungsten tellurite glasses for broadband near-infrared optical fiber amplifiers and tunable fiber lasers. *RSC Adv.* **11**, 27992–27999. https://doi.org/10.1039/d1ra05269a (2021).

76. Yang, X. L., Wang, W. C. & Zhang, Q. Y. BaF_2 modified Cr^{3+}/Ho^{3+} co-doped germanate glass for efficient 2.0 μm fiber lasers. *J. Non-Cryst Solids*. **482**, 147–153. https://doi.org/10.1016/j.jnoncrysol.2017.12.031 (2018).
77. Xia, L., Zhang, Y., Shen, X. & Zhou, Y. Broad and flat dual-band NIR luminescence from $Er^{3+}/Tm^{3+}/Ho^{3+}$ tri-doped tellurite glass. *Opt. Lett.* **46**, 853–855. https://doi.org/10.1364/OL.418971 (2021).
78. Huang, F., Cheng, J., Liu, X., Hu, L. & Chen, D. Ho^{3+}/Er^{3+} doped fluoride glass sensitized by Ce^{3+} pumped by 1550 nm LD for efficient 2.0 μm laser applications. *Opt. Exp.* **22**, 20924–20935. https://doi.org/10.1364/OE.22.020924 (2014).

Acknowledgements
Publication co-financed by the funds granted under the Research Excellence Initiative of the University of Silesia in Katowice.

Author contributions
W.A. Pisarski originated the research concept and interpreted results. J. Pisarska, M. Kuwik, M. Kochanowicz, J. Żmojda, P. Miluski, M. Wełna carried out most of the experiments and data analysis. J. Pisarska, J. Dorosz, D. Pugliese, D. Dorosz discussed the results and commented on the manuscript. W.A. Pisarski wrote the manuscript.

Funding
This research did not receive funding.

Declarations

Competing interests
The authors declare no competing interests.

Additional information
Correspondence and requests for materials should be addressed to W.A.P.

Reprints and permissions information is available at www.nature.com/reprints.

Publisher's note Springer Nature remains neutral with regard to jurisdictional claims in published maps and institutional affiliations.

Open Access This article is licensed under a Creative Commons Attribution 4.0 International License, which permits use, sharing, adaptation, distribution and reproduction in any medium or format, as long as you give appropriate credit to the original author(s) and the source, provide a link to the Creative Commons licence, and indicate if changes were made. The images or other third party material in this article are included in the article's Creative Commons licence, unless indicated otherwise in a credit line to the material. If material is not included in the article's Creative Commons licence and your intended use is not permitted by statutory regulation or exceeds the permitted use, you will need to obtain permission directly from the copyright holder. To view a copy of this licence, visit http://creativecommons.org/licenses/by/4.0/.

© The Author(s) 2026